Reducing Greenhouse Gas Emissions and Energy Costs in Canadian Buildings Using Thermal Mass

by

Alexander Janusz

A thesis submitted in conformity with the requirements
for the degree of Master of Applied Science

Department of Civil & Mineral Engineering
University of Toronto

Reducing Greenhouse Gas Emissions and Energy Costs in Canadian Buildings Using Thermal Mass

Alexander Janusz

Master of Applied Science

Department of Civil & Mineral Engineering
University of Toronto

2019

Abstract

In this thesis, two methods of using the thermal mass in Canadian buildings to reduce operational energy costs and greenhouse gas emissions (GHG) are investigated. The first is cooling commercial buildings with night ventilation. By comparing the climates of Canadian cities to the climates of urban centres with existing night-ventilated buildings, Vancouver and Edmonton were found to have strong night ventilation potential.

The second method investigated is shifting heating demand in electrically heated high-rise residential buildings by varying the thermostat setpoint in order to use less expensive and less GHG-intensive electricity. A representative high-rise residential building was modeled with 16 retrofits in order to evaluate the most important building parameters. Model results indicated annual electricity cost savings of up to $34,000 and GHG savings of 20 Tonnes eCO_2 in a 300-unit building. Further, findings indicated financial savings would increase if residential users were charged for their peak electricity demand.

Acknowledgments

I would like to thank my supervisor, Professor K.D. Pressnail, for this outstanding opportunity to learn about sustainable buildings under his guidance. His experience and advice were invaluable in formulating the study design and direction, editing, data analysis, and interactions with industry. His encouragement to follow my passions and his dedication to improving my skills as a researcher made this experience among the most challenging and rewarding of my life.

I would also like to thank Professor R.D. Hooton for his comments and insights, and Professor M. Touchie for her encouragement before I started my masters, and for the opportunities she has given me since.

I'm also very fortunate to have had the company and support of many exceptional people along the way including my colleagues Masih, Jamie, Helen, Bowen, Amy, and Jay, my teammates in UTFLL, my sister Carolyn, my brothers Adam and Nick, my friends Max, Adnan, Lika, and others in Toronto and beyond.

Finally, I'd like to thank my parents for their unwavering love and encouragement throughout my education, and for teaching me the most important lesson by example: Always busy, and yet always ready to lend a hand. . . or a shovel.

Table of Contents

List of Tables

List of Figures

List of Appendices

List of Acronyms

ACH - Air changes per hour

AEF - Average Emission Factors

ASHRAE - American Society of Heating, Refrigeration and Air-Conditioning Engineers

CDH - Cooling Degree-Hours

$CDH_{18.3°C}$ - Cooling Degree-Hours Calculated Relative to an 18.3°C Base Temperature

CCP - Climatic Cooling Potential

COP - Coefficient of Performance

CWEC - Canadian Weather Year for Energy Calculation

CWEEDS - Canadian Weather Energy and Engineering Datasets

EPW - EnergyPlus Weather (Data)

EPS - Expanded Polystyrene

IESO - Independent Electricity System Operator

GHG - Greenhouse Gas (Emissions)

HVAC - Heating, Ventilation and Air-Conditioning

HOEP - Hourly Ontario Electricity Prices

HRV - Heat Recovery Ventilation

MEF - Marginal Emission Factors

NRCan - Natural Resources Canada

StatsCan - Statistics Canada

TABS - Thermally Activated Building Systems

TOU - Time-Of-Use (Electricity prices)

US DOE - United States Department of Energy

Chapter 1
Introduction

1.1 Background

At the 2016 United Nations 21st Conference of Parties, 195 countries agreed to reduce Greenhouse Gas (GHG) emissions to well below 1990 levels in order to limit global warming to below 2ºC. To that end, it is important to consider that heating and cooling buildings significantly contributes to global energy use and GHG emissions. In Canada, buildings account for approximately 27% of secondary energy use (NRCan 2019) and 19% of GHG emissions (Environment and Climate Change Canada 2019). Reducing the GHG emissions associated with heating and cooling is one of the most financially attractive options for generally reducing GHG emissions (Enkvist et al. 2010). Common methods for achieving this goal include using more efficient heating and cooling systems, switching to less GHG-intensive fuels, or reducing heating and cooling loads through building envelope improvements.

In Western European countries such as Germany and the United Kingdom, "thermal mass" (alternately referred to as "thermal inertia") is widely used to improve heating and cooling performance. Thermal mass refers to the amount of thermal energy a material can store for a given temperature change (J/kg˚C or J/˚C). Depending on the application, thermal mass may allow heating and cooling systems to operate more efficiently, allow systems to use electricity when it is cleaner and cheaper, or enhance the passive heating and cooling of buildings.

Although all buildings have thermal mass inherently, the purposeful use of thermal mass is much less common in Canada than in Western Europe. Some strategies that have been widely used in Europe appear to have been used and documented in just a handful of Canadian buildings. In addition, although the use of thermal mass has been established in Western Europe, thermal mass strategies are impacted by weather, building construction, and fuel type and prices. Thus, it is useful to examine whether the use of thermal mass is suited to buildings in Canada.

Two strategies for using thermal mass in buildings are explored in this thesis: cooling with night ventilation, and shifting heating demand using variable suite-level temperature control. Although these methods have been studied in Western European countries, this work is unique in that it

analyzes how their performance would be affected by the weather, types of building construction, electricity costs, and electricity GHG intensity in Canada.

1.1.1 Thermal Mass in Buildings

The thermal mass of an object is a property that describes how much thermal energy can be stored for a given temperature change. While all materials in a building have thermal mass, denser materials tend to have more. In the case of buildings constructed with concrete floor slabs or masonry walls, the structure is generally the greatest source of thermal mass. Although there are numerous thermal mass technologies such as phase-change materials, the use of concrete is more common and will be considered in this research.

The thermal mass in a concrete structure is typically very large relative to daily heating and cooling needs. Thus, the rate of heat transfer to and from the concrete structure is generally the limiting factor in thermal mass performance. In some buildings, thermal mass absorbs and emits heat passively, by convective and radiant heat transfer. However, the rate of passive heat transfer can be quite slow. Therefore, to improve the transfer of energy to and from the thermal mass, active strategies of heat transfer are utilized including using embedded air channels, embedded water pipes, or electric heating traces.

Thermal mass can be used to reduce the energy required for heating and cooling buildings. Since thermal mass can store thermal energy, it can be charged or discharged at an optimal time. For example, for buildings which are cooled with night ventilation or Thermally-Activated Building Systems (TABS), thermal energy is accumulated in concrete floor slabs during the day and then purged at night, when cooling equipment runs more efficiently. In cold climates, such as those in Canada or parts of Europe, buildings with high thermal mass walls and floors also tend to use less heating energy—approximately 4 to 8% annually (Aste et al. 2009; Di Placido 2014). Thermal mass can also be used to take advantage of hourly variations in electricity prices or GHG emissions. In this case, GHG emissions and heating costs can be reduced even if the energy used or the heating system efficiency are unchanged. Greater benefits will be attainable if the hourly variations in electricity prices and GHG emissions are large.

1.1.2 Thermal Mass Applications in Europe and Canada

Several large research programs in Europe tested a variety of thermal mass strategies in dozens of low-energy buildings (International Energy Agency 1998; Voss et al. 2007). In Britain, night ventilation and concrete core conditioning are frequently used by building owner-operators keen to save on energy bills and boast their green credentials (De Saulles 2006). In Germany, guidelines for cooling load calculations account for thermal energy storage by dynamically evaluating building performance over 14 days (VDI 2015).

By contrast, in Canada, some types of thermal mass strategies have rarely been attempted. Literature research done for this thesis found reports of only two Canadian high-rise buildings that used night ventilation. Caution must be exercised, however, in applying existing research on thermal mass to the Canadian buildings, as thermal mass strategies that work well in Europe may not be well-suited to Canada. This is because Canada has: lower energy prices than Europe; different types of building construction than Europe; and a wide variety of climates. All of these considerations influence the effectiveness of thermal mass strategies.

1.2 Proposed Strategies

This research considers two thermal mass strategies in the Canadian context. The first strategy, night ventilation, is an efficient method of cooling office buildings. The second strategy, using variable suite-level temperature control to shift heating demand in electrically heated high-rise residential buildings, shifts heating demand to times of day when electricity is less GHG-intensive and less expensive.

In a night-ventilated building, thermal mass absorbs heat during the day, then at night the building is flushed with cool outdoor air. Night-ventilated buildings are typically purpose-designed or retrofitted to facilitate cooling by night ventilation, since using typical ventilation systems would result in poor cooling efficiency. Purpose-designed, night-ventilated buildings typically utilize operable windows and exhaust stacks to minimize or eliminate fan usage. Cooling at night not only saves energy, but also reduces stress on the electrical grid in the mid-afternoon, when demand for electricity is often the greatest. Even though Canada has a relatively cool climate, commercial buildings could still benefit from this technology as they require cooling much of the year.

Variable suite-level temperature control is explored as a means of shifting heating demand in electrically heated high-rise residential buildings in Ontario. Shifting heating demand differs from night ventilation in that the goal is not to improve the energy-efficiency of the building, but rather to shift the electricity demand from peak to off-peak hours in order to use less GHG-intensive and less expensive electricity. Hence, the achievable benefits depend on how GHG intensities and costs of electricity vary during the course of the day. Since Canada has a heating-dominated climate, all high-rise residential buildings require heating. Therefore, even a small benefit could have significant benefits on an urban scale.

1.3 Goals and Methods

This research has two primary goals. Given that the performance of night ventilation hinges on outdoor air temperatures at night, the first primary goal is to assess whether night ventilation is well-suited to the climates of Canadian cities. Since there are many purpose-built night-ventilated buildings in Europe, this research focused on existing buildings instead of modeling a hypothetical building. A metric for the cooling potential of night ventilation from the literature was used to evaluate the climates of locations with existing night-ventilated buildings. Those climates were then compared to the climates of several major Canadian cities to identify whether they are promising locations for the strategy.

The second primary goal of the research is to examine the potential of using variable suite-level temperature control combined with building thermal mass to shift heating demand in existing 1960s and 1970s era high-rise residential buildings in Southern Ontario. Specifically, the second goal is to identify the potential electricity cost and GHG emission savings attainable by shifting heating demand in electrically heated high-rise residential buildings. Southern Ontario was selected as the location of study because buildings, climates, and electrical grid characteristics vary substantially across Canada, and this region is densely populated and is home to around 35% of Canada's population (Statistics Canada 2019). The analysis used a detailed, calibrated model of an existing high-rise residential building in Toronto as a starting point. Toronto is located in Southern Ontario and is the most populous city in Canada. The subject building is typical of high-rise residential buildings constructed in the 1960s and 1970s, and therefore represents approximately 25% of housing units in Toronto (Touchie 2014). Since the characteristics of buildings can be changed through retrofits, 16 combinations of retrofits to the

heating system, interior finish, envelope, and ventilation system were considered. The GHG emission reductions and financial savings were evaluated using electricity prices and emission factors specific to Ontario.

1.4 Thesis Structure

This thesis contains two papers. In the first paper, which comprises Chapter 2, the potential for cooling office buildings in Canada with night ventilation is explored. In the second paper, which forms Chapter 3, models of an existing high-rise residential building with various combinations of retrofits are used to explore the potential of shifting heating demand in order to reduce electricity costs and GHG emissions. Chapter 4 summarizes the findings contained in these two papers and discusses pertinent areas which would benefit from further research.

Chapter 2
Assessing the Potential of Using Night Ventilation and Thermal Mass to Temper Cooling Loads in a Heating Dominated Climate

This chapter addresses the question of whether it is possible for office buildings in Canada to "cool themselves" by using night ventilation and thermal mass to provide low-energy or passive cooling.

In Canada, cooling accounts for approximately 4% of energy use in commercial buildings (NRCan 2011). Moreover, Canada's climate is changing: On average, Canada warmed by 1.5°C between 1950 and 2010 (Warren and Lemmen 2014), and cooling degree days are projected to increase by between 30% and 100% by the middle of this century (Wilson and Marchand 2016). Further, cooling loads continue to drive peak electricity demand in Ontario. However, more efficient cooling methods could reduce cooling energy usage and peak demand.

Night ventilation makes use of daily ambient air temperature variations to cool buildings. At night, ventilation with low-temperature air cools the building interior, which can then absorb heat the following day. Since the cooling and heating occur at separate times, energy storage is essential to this process. The energy storage is supplied by "thermal mass" materials such as concrete or phase change materials. Office buildings require cooling much of the year due to internal gains and are ideally suited to night ventilation because they are empty overnight. Night ventilation is attractive both in terms of its low energy requirement and its favorable grid interaction, which capitalizes on electricity at night when the grid is under less stress and there is often an excess of renewable power available.

The known benefits of night ventilation are numerous, including the utilization of smaller, more economical mechanical systems, and cooling energy savings. However, night-ventilated cooling also has unique challenges which must be addressed, including acoustics issues due to hard surfaces, fire protection, ventilation control in open spaces, dust and moisture entering buildings at night, and optimizing building design for natural ventilation (Pfafferott 2004).

There have been many large night-ventilated buildings reported in European countries, most notably in Germany and the United Kingdom. In Canada however, night ventilation has received limited exposure. In this study the suitability for night ventilation in Canada is assessed by

comparing the climates of places with existing night-ventilated buildings to the climates of Canadian cities. A short literature review and summary of the operating principles of night ventilation are first presented to assist the reader with understanding this technology.

2.1 Night Ventilation Research

Night ventilation has been an active area of research for several decades. Baruch Givoni, who is renowned for his research on passive cooling, experimented with night ventilation as early as 1962 (Givoni 1994). In the 1970s and 1980s, a growing energy consciousness and the popularization of air-conditioners spurred widespread research into night ventilation and other passive cooling strategies (Agas et al. 1991).

The 1990s was a prolific period for major international low-energy cooling research and demonstration projects. By this time night ventilation was conceptually well understood, so the general goal of these large projects was to make night ventilation and other low-energy cooling technologies more widely accessible by establishing user-friendly tools and design techniques, and by conducting case studies for passive cooling. The European Commission Joule II project "PASCOOL" (1992-1995) (Allard et al. 1996; Blondeau et al. 1997) was one of the first such projects, and it was soon followed by the International Energy Agency (IEA) project "Annex 28: Low-Energy Cooling" (1993-1997). Annex 28 researchers created design methods and user-friendly software, published dozens of low-energy cooling case studies (International Energy Agency 1995a; International Energy Agency 1998), and spawned several conferences and books (Tassou 1998; Zimmermann 2003). Subsequent projects included "NatVent", a seven-country pan-European project (1994 to 1998) (NatVent 1998), and IEA "Annex 35: HybVent" (1998-2002) (Heiselberg 2002).

In 1995, The German Federal Ministry for Economic Affairs and Energy launched the intensive research and demonstration program entitled "EnBau". The goal of the program was to showcase market-ready, low-energy building technologies. EnBau entailed the construction and monitoring of 22 low-energy demonstration buildings, 17 of which utilized night ventilation as part of their cooling strategy (Voss et al. 2007). Entrance requirements for the program included a projected annual primary energy use of less than 100 kWh/m^{2}a as well as excellent thermal comfort and visual conditions. The project provided no subsidies, so all the buildings involved in it were completed under realistic economic conditions. Once the buildings were completed, they were

monitored by university researchers. In the United Kingdom, during the same period, extensive research and significant industry experience advanced the design methods and performance of night ventilation systems (De Saulles 2006).

More recently, night ventilation research has largely focused on hybrid control strategies, the use of phase change materials, and the determination of more accurate heat transfer coefficients through computer simulation and experimentation (Solgi et al. 2018).

While studies have looked at the potential for cooling with night ventilation in Europe, China, and the United States (Axley 2001; Artmann et al. 2007; Liu et al. 2017), a review of the literature revealed no evaluations of the potential for night ventilation strategies in Canada.

2.2 Operating Principles

In a night-ventilated building, at night fans or stack action are used to draw cool, outdoor air through the building. The night air cools the thermal mass in the building, which absorbs heat the following day. For optimal cooling to occur, the thermal mass should be in direct contact with indoor air. Lightweight coverings, such as suspended acoustic tiles on ceilings, greatly reduce heat transfer, in turn reducing thermal mass performance. Instead of lightweight coverings, dense plaster coatings and paint are generally used to provide a pleasing surface finish without significantly inhibiting heat transfer.

Night ventilation can be used in both residential and commercial buildings. As most residential buildings have limited solar loads and internal gains, passive night ventilation and heavy construction can maintain comfortable indoor air temperatures in hot climates (Geros et al. 1999). Because of this, some engineers suggest that night ventilation should be used to future-proof homes from the demands of a warming climate (CIBSE 2005; Hacker et al. 2007).

Commercial buildings have larger cooling loads and more stringent thermal comfort requirements than residential buildings, so they generally use a combination of mechanical and passive night ventilation, and the undersides of heavy ceiling slabs are exposed. It is generally accepted that this method can offset peak cooling loads of up to 25 W/m^2 (International Energy Agency 1995b; Blondeau et al. 1997; Van Paassen et al. 1998; De Saulles 2005) and daily coolin loads of 150 to 250 Wh/m^2 if night-time temperatures are sufficiently cool (Pfafferott et al.

2003). In cases where night-time temperatures are not consistent, night ventilation is supplemented by other systems, such as evaporative cooling, ground-to-air heat exchangers or traditional chillers. Despite the apparent redundancy of having two types of cooling systems, utilizing thermal mass in buildings reduces the peak cooling load, resulting in smaller and less expensive cooling systems (Voss et al. 2007).

Although night ventilation is conceptually simple, to cool efficiently with night ventilation requires an integrated building design. While it is possible to distribute the ventilation air at night with typical ducts, the system efficiency would be similar to that of traditional air-conditioners. More efficient designs reduce fan losses by using larger air delivery ducts or by drawing outdoor air directly into the building through exterior windows.

Figure 1 shows an example of a common design for a night-ventilated high-rise building that uses an atrium as an exhaust plenum (Wagner et al. 2007). In this building, automated windows separate the atrium from the offices so they can be compartmentalized during the day, while at night the exterior and interior windows can be opened to enhance airflow by stack action.

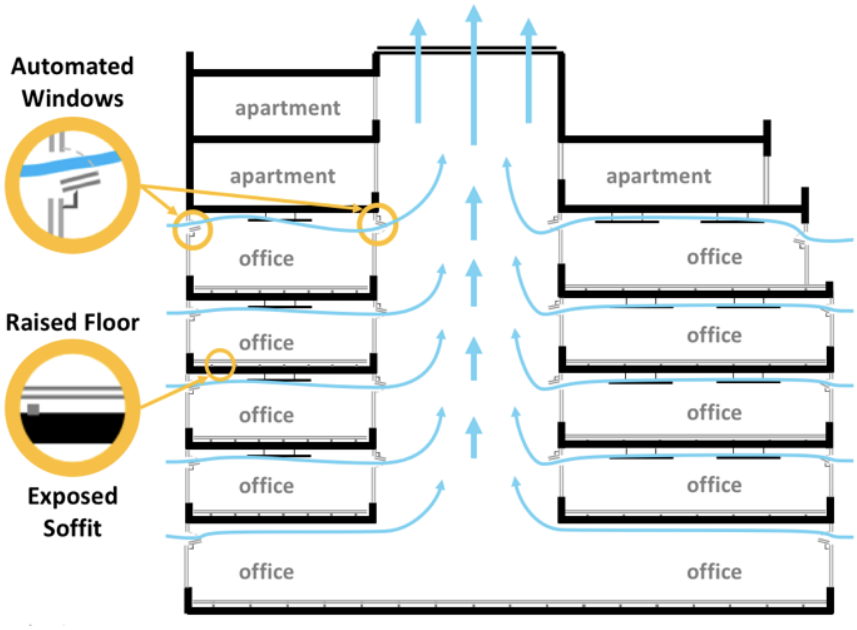

Figure 1 : Schematic of a Typical Night-Ventilated Office Building*

* Adapted from Wagner et al. (2007)

Cooling with night ventilation has climatic requirements, particularly the need for night air to be sufficiently cool. In hot-humid climates, the diurnal swing is small, reducing the potential for night ventilation (Givoni 1994). However, even places which have hot and humid summers frequently experience significant periods during the shoulder season when night ventilation is more effective (O'Brien et al. 2015).

2.2.1 Cooling Capacity

The cooling power of thermal mass depends on its material properties, the rate of direct heat transfer from occupants and equipment by thermal radiation, and the rate of indirect heat transfer by convection. Assuming that concrete is being used as the thermal mass, improving convective heat transfer is the most effective means of these three to increase cooling capacity. Improving the conductivity or density of the concrete has a limited effect, as the thermal resistance within a typical concrete slab is only 1/10th that of the thermal resistance at the slab surface attributable to convective transfer and radiation exchange. Further, the radiative transfer at the surface of ceilings cannot be changed significantly as the emissivity of common construction materials is high to begin with, and contouring the ceiling surface does not improve radiant heat transfer (Döering et al. 2013).

The two main methods of enhancing convective heat transfer are to increase surface area and to increase the convective heat transfer coefficient. Surface area can be increased with additional high thermal mass surfaces, such as exposed concrete floors, or with interior partition walls made from concrete wallboard or drywall containing phase-change material (Landsman 2016). However, many night-ventilated buildings are open-plan in order to enhance airflow, which limits the potential of using partition walls to provide thermal mass. To address this limitation, the surface area of the concrete slabs can be increased by creating a ceiling with a profiled surface, such as fluted metal decking, waffle slabs, or ribbed slabs. While profiled ceilings may have 2 to 3 times the surface area of a flat surface, they only provide approximately 25% more cooling capacity, as the convective transfer from vertical surfaces is half that of horizontal surfaces, and the extra surface area does not increase radiant transfer (International Energy Agency 1995b; Döering et al. 2013).

Since profiling the ceiling slab can only achieve about a 25% increase in cooling capacity, a raised floor is often used as an air supply plenum to further enhance heat transfer. This

effectively doubles the surface area of the slabs, and the turbulence in the plenum enhances convective transfer. This results in a cooling capacity of approximately 40 W/m^2 (De Saulles 2005). Similarly, pre-fabricated hollow-core slabs with air channels inside may be considered. Although hollow-core slabs and floor plenums do improve thermal performance, indoor air quality experts view them with caution, as such spaces tend to collect dust and are difficult or impossible to clean (ASHRAE 2009).

2.2.2 Night Ventilation Cooling Efficiency

Equation 2-1 can be used to calculate the coefficient of performance (COP) for fan-assisted night ventilation (Barnard 1996).

$$COP_{NV} = \frac{\text{Cooling Energy}}{\text{Fan Energy Input}} = \int \frac{Q \cdot \rho \cdot c_p \cdot (T_r - T_a)}{Q \cdot \Delta P / \eta_f} \, dt \qquad [2\text{-}1]$$

Where:

COP_{NV} = Coefficient of Performance for Fan-Assisted Night Ventilation
Q = air supply rate (m^3/s)
ρ = density of air (kg/m^3)
c_p = specific heat capacity of air (J/kgK)
T_r = space air temperature (°C)
T_a = ambient dry bulb temperature (°C)
ΔP = System pressure drop (Pa)
η_f = fan efficiency (0.0 to 1.0)
t = time during which night ventilation occurs

The system pressure drop and fan efficiency are the easiest of these variables to change. While night-ventilated buildings with fans to assist airflow might theoretically have a COP_{NV} as high as 25 (Barnard 1996), the reported COPs for fan-assisted night-ventilated buildings in the EnBau program ranged between 4.5 and 14 (Voss et al. 2007). The building with a COP_{NV} of 4.5 relied on a ducted supply with a ventilation energy intensity of 0.45 W/m^{3}h (Pfafferott et al. 2003). Some office buildings are specially designed to facilitate night ventilation by stack action. One example is the 8,900 m^2 building "KfW Osterkade", which was shown in Figure 1.

In a given building, changes in COP_{NV} are primarily due to variations in outdoor air temperature and ΔP. However, when comparing different buildings, other variables also need to be considered. The temperature difference between the air entering and leaving the building is affected not only by ambient air temperature, but also by surface temperatures, airflow patterns, and building design features such as the surface area of the thermal mass and the volume of the room (Barnard 1996; Artmann et al. 2010).

2.3 Applicability to the Canadian Climate

2.3.1 Methods of Evaluating Night Ventilation Cooling Potential

The effectiveness of night ventilation depends on three parameters: building design, control strategy, and climate. Since building design and control strategy are not location specific, this research aimed to isolate the effect of climate in assessing the potential for night ventilation in Canadian cities.

Building energy simulation was initially considered for evaluating night ventilation, as it is a commonly used method for such evaluations. It was ultimately rejected because the results of a building energy simulation depend on all three categories of parameters, which makes it challenging to generally address the suitability of the Canadian climate for night ventilation. With building energy simulations, it would be difficult to avoid making building-specific assumptions that would limit the generality of results. For example, previous researchers set out to create a highly simplified pre-design tool called “Nitecool”. However, Nitecool still required eight building variables to specify a basic office cell (International Energy Agency 1995a). Additionally, night ventilation is also affected by building details not accounted for by those eight variables, such as ventilation supply configuration (Blondeau et al. 1997; Artmann et al. 2010).

While there are ways to handle these challenges with building energy simulation, an entirely different route was taken for this work by considering the climate of existing night-ventilated buildings that have been reported in the literature. The selected buildings are all post-construction and reported to be operating successfully. The cooling load of the buildings was generally not reported, but the buildings selected are all low-energy institutional or commercial buildings built without subsidies. Thus, they can be seen to represent a range of designs that

could possibly be built in Canada. To compare the climates in which existing buildings are located to the climates of Canadian cities, suitable metrics were needed to represent the daily cooling load and night ventilation cooling potential. In this study, the metric selected for cooling load was Cooling Degree-Hours (CDH). While solar gains and internal loads are also important factors in determining building cooling loads, it is difficult to also incorporate these factors without compromising generality. While the balance point temperature of buildings varies, 18.3°C is typically used when calculating CDH, and approximates the temperature at which heat removal becomes necessary in a large building (Eto 1988).

To represent the cooling potential of night ventilation, several night ventilation metrics from the literature were considered, and a quantitative metric called "Climatic Cooling Potential" (CCP) was selected (Artmann et al. 2007). CCP minimizes building assumptions, which increases its generality. As shown in Figure 2, CCP is similar to CDH in that they are both an integral of a temperature difference over time and have units of °C-h.

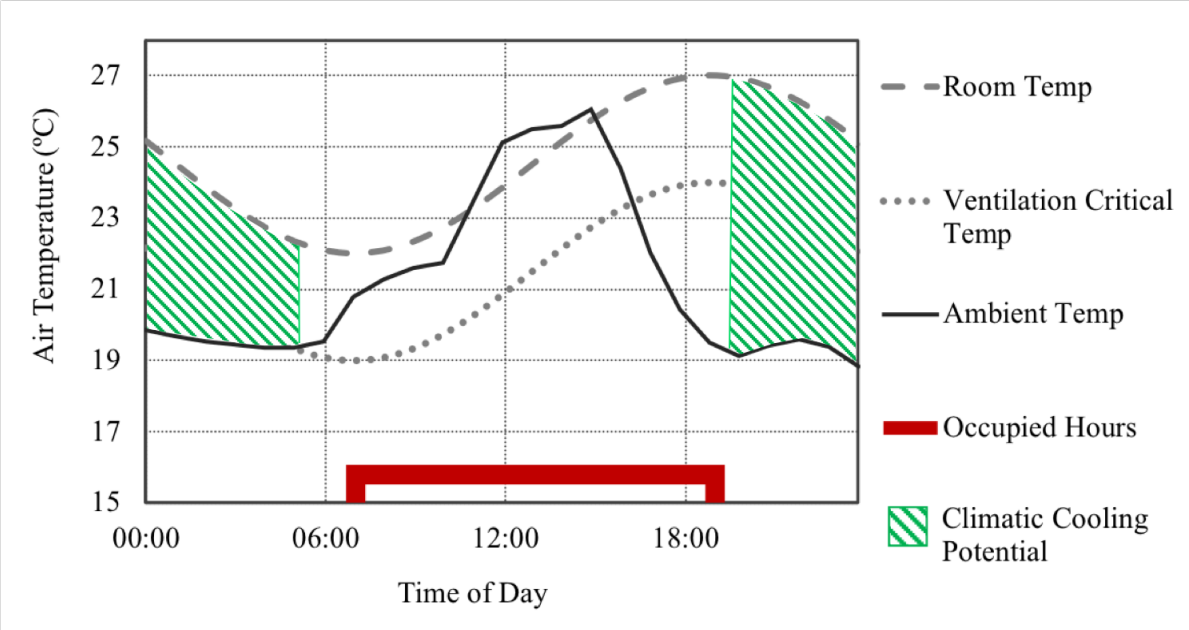

Figure 2 : Example of the Climatic Cooling Potential (CCP) Calculation*

*Adapted from Artmann et al. (2007)

However, the CCP calculation differs from the CDH calculation in two key ways:

First, when calculating CCP, the base temperature is not a constant "balance point" temperature. Instead, the base temperature represents the temperature of the surfaces in the building and is assumed to vary sinusoidally. Each day, the indoor air temperature is assumed to reach a maximum temperature of 27°C at 7 pm, and to reach a minimum of 22°C at 7 am.

Second, CCP is not measured for the entire day. Rather, the cooling potential is only integrated during the designated night ventilation period, between 7 pm and 7 am. But, even then, ventilation cooling potential is only integrated if the outdoor air temperature is more than 3°C cooler than the assumed building temperature. The difference of 3ºC is stated to be the "critical temperature" necessary for effective night ventilation (Blondeau et al. 1997).

Much like heating degree-days can be used to estimate the energy required to heat a building, CCP can be used to estimate the cooling energy available from night ventilation (Artmann et al. 2010). Consider an illustrative calculation of the cooling capacity on a per-m^2 of floor area basis for a simple building. For this example, it is assumed that the building has 3 m high ceilings, is ventilated with 5 air changes per hour (ACH) during the night, and that the night has 70°C-h of cooling potential. To account for imperfect heat transfer between the building and the ventilation air, a ventilation efficiency factor, η_{NV}, is used. The calculation of η_{NV} in Equation 2-2 accounts for the fact that air leaving the building will not be at the same temperature as the building thermal mass.

$$\boldsymbol{\eta_{NV} = {\mathbf{T}_e - \mathbf{T}_a}/{\mathbf{T}_s - \mathbf{T}_a}} \qquad [2\text{-}2]$$

Where:

η_{NV} = Ventilation temperature efficiency (°C)
T_e = Exhaust air temperature (°C)
T_a = Ambient air dry bulb temperature (°C)
T_s = Slab surface temperature (°C)

Experiments and analytical calculations indicate that η_{NV} is typically between 0.4 and 0.8, and is a function of air exchange rate and building characteristics (Barnard 1996; Artmann et al. 2010). For this example, 0.6 is assumed:

$$\frac{E_{NV}}{A} = CCP \cdot (ACH \cdot H \cdot \rho) \cdot \eta_{NV} \cdot c_p \qquad [2\text{-}3]$$

$$\frac{E_{NV}}{A} = 70°\text{Ch} \cdot {}^{5}/_{h} \cdot 3m \cdot 1.2\frac{kg}{m^3} \cdot 0.6 \cdot 0.278\frac{Wh}{kg°C}$$

$$\frac{E_{NV}}{A} = 210\,\frac{Wh}{m^2}$$

Where:

E_{NV} = Cooling Energy (Wh)
A = floor area (m^2)
CCP = Climatic Cooling Potential (ºCh)
ACH = air changes per hour (1/h)
H = height of building ceiling (m)
ρ = density of air (kg/m^3)
η_{NV} = Ventilation temperature efficiency (°C)
c_p = specific heat capacity of air (Wh/kg.°C)

Thus, using Equation 2-3, it is calculated that 70ºC-h is necessary to remove 210 Wh/m^2 of accumulated heat gains.

However, the CCP metric does have several limitations. One limitation is that the calculation assumes the same building temperature profile every day, regardless of building design or the ambient air temperature on a given night. Since the building temperature profile is part of the CCP integral, it has a strong impact on the predicted CCP. There are many reasons that the temperature profile of a building would diverge from the assumed profile, in which case CCP will no longer provide an accurate assessment of cooling potential. One instance when this assumption could be invalid is if a night remains warm until early morning. The temperature profile used in the CCP calculation assumes that the temperature of the hypothetical building decreases through the night, whereas a real building would remain warm. This means that for a

real building, still being warm, some useful cooling potential would exist in the early morning. However, the CCP calculation would indicate that the building is already too cool, and thus no cooling potential exists.

Another important scenario that would cause the temperature profile of a real building to diverge from the assumed profile, is if a building was maintained at a higher temperature than between 22ºC and 27ºC, as assumed in the CCP calculation. For example, in a hot country an office building might be maintained at 25ºC during working hours, and then allowed to drift up to 35ºC when unoccupied at night. Such a building would have much more cooling potential than that indicated by the CCP calculation. While having several temperature profiles or a dynamic profile might improve accuracy, it would require additional building-specific assumptions, and thereby reduce the generality of CCP.

Another limitation of the CCP metric is that the impacts of ambient relative humidity are not considered. When calculating CCP, it is assumed that all night air, if sufficiently cool, is useful for cooling. However, bringing night air that is at a high relative humidity into a building might result in moisture related problems. The relative humidity in buildings is commonly maintained between 30% to 60% for occupant comfort, to minimize indoor air contaminants such as bacteria or mites, and to reduce the chances of condensation-related structural damage (Arundel et al. 1986; Tran 2013). Further, if the building is climate-controlled during the day, extra moisture brought in with night ventilation may be an additional latent load on the building air-conditioning system. Reports of night-ventilated office buildings in moderate climates indicate that humidity is not typically accounted for in the night ventilation controls (Brager et al. 2007). However, one exception is the night-ventilated Renson office building in Belgium, which is reported to be automated such that night ventilation is halted if indoor relative humidity rises above 70% (Breesch 2006). Thus, even in moderate climates, it may be necessary to limit night ventilation if ambient humidity levels are too high.

2.3.2 Evaluating the Night Ventilation Potential in Canadian Cities

The mean daily $CDH_{18.3°C}$ and CCP were calculated for the climates in the locations of existing night-ventilated buildings and for the climates of several Canadian cities. CCP and $CDH_{18.3°C}$ were calculated for the month of July, as July is generally the hottest month in Canada and Europe, and thus is the limiting case for cooling systems. The mean $CDH_{18.3}$ were based on

ASHRAE climatic design conditions data (ASHRAE 2013). The mean CCP were determined either by performing hourly calculations based on "typical weather" data, as described in Artmann et al. (2007), or by using compiled Meteonorm data obtained from the same publication. These data are all based on long-term historical meteorological conditions, mostly between 1960 and 1990.

One shortcoming of the presentation of data in Artmann et al. (2007) is the low resolution of the results. This meant it was impossible to distinguish the elevated temperatures due to heat island effect in the centres of large cities. To capture such effects, this work used data from downtown weather stations for large cities. For the cities in the United Kingdom, EnergyPlus Weather (EPW) data were sparse. Thus, the approach for cities without EPW data was to use EPW files from the nearest airport to determine which year the "typical" July weather was taken from, and then use concurrent data from the weather station in the city to perform the CCP calculations. EPW data were available for the large cities in Germany and the United States. Compiled data from Artmann et. al (2007) were used for smaller German cities without EPW files, such as Creuzberg. Good agreement was observed between the compiled data and the calculations performed with the EPW files when considering small cities such as Bremen, DE. For Canadian cities, the typical month was determined from Canadian Weather Year for Energy Calculation (CWEC) files. CWEC data from the nearest station were used directly for Ottawa, Quebec City and Winnipeg, while concurrent Canadian Weather Energy and Engineering Datasets (CWEEDS) from a station closer to the urban core were used for Toronto, Vancouver, and Edmonton.

This CCP data and $CDH_{18.3°C}$ data for Canadian Cities and for the locations of existing buildings were then plotted in Figure 3. In this figure, in addition to the climatic data, the size and colour of the dots also convey information about the existing buildings. The size of the circles is proportional to the floor area of existing buildings, while the colour of the circles indicates the type of building cooling system. In the case of Canadian cities, since the circles represent potential locations for night-ventilated buildings, the colour of the circles is the same for all Canadian cities, and the size was made equivalent to a 5000 m^2 building in order to provide reference. The data sources for each circle are provided in Appendix A.

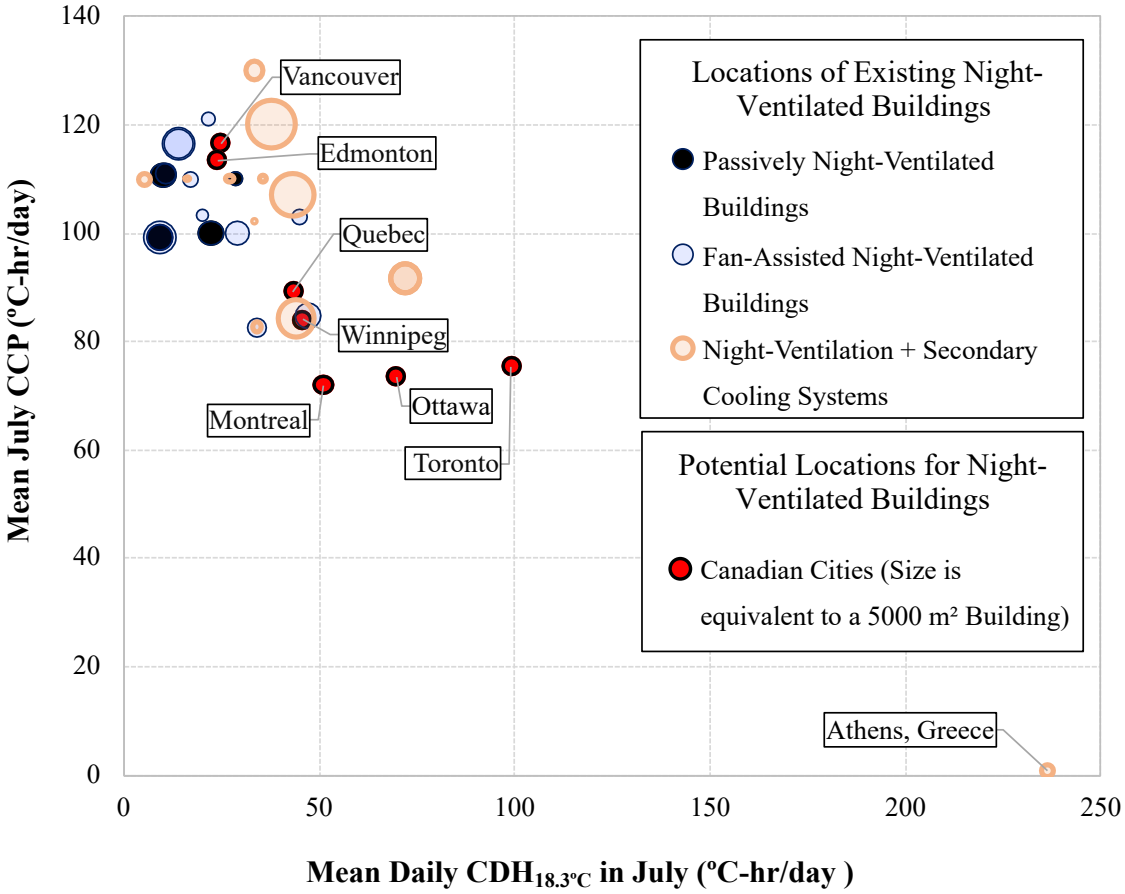

Figure 3 : Climatic Cooling Potential (CCP) and Cooling Degree-Hours ($CDH_{18.3°C}$) for Canadian Cities, and for Cities Abroad with Existing Night-Ventilated Buildings*

*The area of the circles represents the conditioned floor area of the buildings.

Figure 3 shows that the climate of cities in Canada is more variable with respect to CCP and CDH than the climate of cities in Europe and the United States with existing night-ventilated buildings. Some cities like Edmonton and Vancouver have abundant climatic cooling potential, while other cities such as Ottawa, Montreal, and Toronto typically have less climatic cooling potential than the location of existing buildings identified in the literature. However, this does not necessarily mean that Montreal or Toronto are too warm to benefit from night ventilation, as Montreal and Toronto still have significant CCP on average. The majority of the building locations represented in Figure 3 are either in Germany or the United Kingdom, which have relatively moderate climates. In fact, among the building locations represented in Figure 3 are Frankfurt, Germany and London, England which are in the warmest areas of those countries (Artmann et al. 2007). Thus, night-ventilated buildings might well be suitable in warmer climates

still, but to date this technology has been employed primarily in the United Kingdom and Germany.

The potential for night ventilation in warmer climates is highlighted by the circle in the bottom-right corner of Figure 3 labelled “Athens, Greece”. The circle represents a single building in Athens which was cooled with a combination of air-conditioning and night ventilation. Reports of this building indicated that when Athens had nearly zero CCP, it maintained a daytime indoor air temperature of 25°C and the use of night ventilation reduced annual cooling energy by 50% compared to cooling with air-conditioning alone (Geros et al. 1999; Build Up 2010). The reason the Greek building was able to achieve cooling despite having a CCP of nearly zero is thought to be due primarily to the divergence between the actual temperatures within the building and the temperature profile assumed in the CCP calculation, as previously described. Records for this building show that it reached high temperatures in the evening and remained quite warm throughout the night. Thus, the real building had significant cooling potential that wasn’t captured by the CCP calculation.

The grouping of the different types of night ventilation systems in Figure 3 indicate that there is a climatic limitation beyond which it is difficult to cool a building solely with night ventilation. There is a cluster of black and blue circles which represent locations with buildings cooled solely by passive or fan-assisted night ventilation. The locations of these cities have an average CCP of greater than 90 and less than 30 $CDH_{18.3°C}$. Based on this, it appears that the climates of Vancouver and Edmonton have the potential for purpose-built office buildings to be cooled solely with night ventilation. Conversely, although the climates of Toronto, Ottawa, and Montreal have significant cooling potential, it appears that currently even an appropriately designed office building in these cities will require other forms of supplementary cooling.

2.4 Conclusions

Night ventilation is a cooling strategy that necessitates an integrated building design, but relies on simple and robust technologies. Extensive international studies, demonstration projects, and commercial projects have indicated that it is a mature and effective cooling strategy. It is not without challenges, but most of these are manageable if care is taken during the design process. However, the challenges associated with bringing untreated air into the building at night are not

easily resolvable. If the climate prohibits this process because the air contains too much moisture, dust, or pollution, night ventilation may not be a good solution.

The data indicate that a well-designed night-ventilated building in cooler Canadian cities, such as Vancouver or Edmonton, might feasibly be cooled year-round with night ventilation. However, warmer cities, such as Toronto and Montreal, will require supplementary cooling. Although Toronto was not found to be as promising as Edmonton or Vancouver with regard to night ventilation, Toronto still had over 50% as much night ventilation cooling potential, as indicated by CCP. However, it is important to recognize that the magnitude of cooling load that can be met by thermal mass and night ventilation has been reported to be limited to 25 W/m^2 with natural convection or 40 W/m^2 with forced convection system, such as with a raised-floor ventilation supply plenum (De Saulles 2005). This means that building designers must also pursue strategies to reduce the cooling load, such as external shading, daylighting, and energy-efficient office equipment.

Chapter 3
Saving Money and Reducing Greenhouse Gas Emissions by Shifting Heating Demand in Retrofitted Concrete High-Rise Residential Buildings in Ontario

The federal Canadian government and the majority of Canadian provinces and cities have set aggressive Greenhouse Gas (GHG) emission reduction timelines. At present, 65% of homes in Canada use natural gas as their primary heating fuel (Statistics Canada 2007). Consequently, building heating is one of the largest contributors to GHG emissions and the Canadian government has identified it as a key focus for GHG reduction (Ministry of Environment and Climate Change 2016). One promising method to reduce the GHG emissions of building heating is to use electric heating systems. In Canada, 80% of electricity is generated from non-emitting sources, making the Canadian grid the second cleanest of the G7 countries (NRCan 2019).

Unlike natural gas, electricity cannot be economically stored for extended periods of time at the grid scale. The consequent lack of energy storage means that electricity generation has to change throughout the day to match demand. In the dense Southern Ontario region, which contains around 35% of Canada's population (Statistics Canada 2019), the base load is met primarily by nuclear and hydroelectric energy, while the peak load is met by more expensive natural gas turbines. This means that electricity at peak hours is both more expensive and GHG intensive than electricity used during off-peak hours (Farhat and Ugursal 2010; TAF 2017).

In addition, the capacity of the electrical grid required is determined by just a few hours of peak electricity demand each year. A larger capacity grid requires more generation sources and equipment, which also means increased maintenance. Ontario has accounted for the increased maintenance cost by charging large industrial and commercial customers for both the electrical energy that they use and their power draw during the five hours of the year when the electrical grid is under the greatest load, which are also known as "peak demand". Historically, it has not been necessary or possible to charge residential customers for their contribution to peak demand, but this is changing. Technologies such as fast-charging electric vehicles and grid-tied solar photovoltaic arrays place significant demands on the grid and are not fairly accounted for by the traditional electricity structures with fixed charges and energy use charges ($/kWh). Further,

smart meter technology enables charges for peak power draws, commonly known as “demand charges”, to be given to residential customers for the first time. This means that, in the future, there may be additional financial incentives for electrically heated buildings to shift their heating demand away from peak hours.

One method of shifting heating demand is to use the building structure for thermal energy storage. Over the past 40 years, many authors have studied how to use building structures to shift heating or cooling demand. When this research began, studies focused on reducing peak cooling in office buildings (Braun 1990). More recently, several major projects conducted by the German government and the International Energy Agency have looked at using the structural thermal mass in buildings to store excess renewable energy as thermal energy (Jensen et al. 2017; Klein et al. 2017). Several researchers have also specifically examined the relationship between the construction of residential towers and how much heating demand can be shifted (Pedersen et al. 2017; Foteinaki et al. 2018).

The present research was undertaken to study the potential of using variable suite-level temperature control combined with building thermal mass to shift heating demand in electrically heated high-rise residential buildings in Ontario. To evaluate the potential of shifting heating demand using thermal mass, an existing Toronto high-rise residential building which is representative of those constructed in the 1960s and 1970s was selected as the subject building. Toronto is a city in Ontario and is the most populous urban centre in Canada. In Toronto, high-rises make up 55% of housing and, of those, approximately half were built in the 1960s and 1970s (Touchie 2014). Further, high-rise residential buildings generally have good potential for load shifting due to their compact geometry and the thermal mass of their concrete construction. Many of these ageing towers will require major retrofits of the mechanical and envelope systems in the near future. Thus, they may be ideal candidates for optimizing the use of thermal mass.

The subject building was modeled using EnergyPlus building energy simulation software (US DOE 2017). This modelling program was used to evaluate the subject building with 16 combinations of interior finishes, building envelopes, electric heating systems, and ventilation systems. The goals of this analysis were to establish which characteristics have the greatest effect on the shifting of heating demand, and to evaluate the consequential financial and GHG emission implications for buildings in Ontario.

While much of the previous research on using thermal mass to shift heating demand has been based on the climates and buildings of Western Europe, this research examined the performance of residential towers in Ontario, which has a colder climate. It also examined the impact of pressurized-corridor ventilation, which is the dominant ventilation method for existing high-rise residential buildings in Canada, but has received limited attention in the literature on load shifting. Lastly, implications for electricity costs and GHG emissions were evaluated using current emission factors and electricity prices for Ontario.

3.1 Methodology

3.1.1 Building Description

The building selected for this case study is typical of high-rise residential buildings built in Toronto during the 1960s and 1970s in that it has a leaky envelope, pressurized-corridor air supply, exposed slab edges, minimal thermal insulation, and no suite-level heating system controls (Touchie 2014). Like many buildings of the period, the structure still has decades of service life remaining, but the energy efficiency and thermal comfort of the building are below modern standards. The annual energy use intensity of the building is approximately 370 ekWh/m^2, which is at approximately the 75th percentile for high-rise residential buildings in Toronto (Touchie 2014). Further, mechanical systems and much of the interior finish may be nearing the end of their service life. When parts of the building are replaced, it creates an opportunity for a larger retrofit such as a renewal of the envelope, interior finishes, mechanical systems, or a combination of these retrofits. In addition to improving energy efficiency, such a retrofit would also provide an ideal opportunity to optimize the building for load shifting.

The study building is 20 stories tall, with an above-ground area of 24,840 m^2, and an additional 3890 m^2 of below-ground parking and storage. It has an inter-floor height of 2.7 m. On each of the floors from 3 through 20, the matching North and South orientations have a gross wall area of 372 m^2/floor and a Window-Wall Ratio of 37%, while the East and West faces have a gross wall area of 242 m^2/floor and a Window-Wall Ratio of 2%. The exterior walls of the building are constructed of non-loadbearing masonry supported on concrete floor-slabs with exposed slab edges. The 102 mm concrete-block exterior walls are insulated with 32 mm Expanded Polystyrene (EPS) insulation and covered with a vented brick façade. Floor slabs are 203 mm concrete, with wood parquet flooring and a plaster ceiling applied directly on the underside of

the slab. Interior partitions are 51 mm of sand-plaster on expanded-metal lath, and demising walls between the units and around the hallway are 102 mm solid concrete-block walls with 25 mm sand-plaster applied to the surface. The composition of the various building elements is summarized in Table 1.

Table 1 : Composition of the Various Building Elements in Subject Building

Description	Composition
Exterior Walls	13 mm Gypsum Board 32 mm EPS Insulation 102 mm Hollow Concrete Block 38 mm vented cavity Exterior Brick
Interior Partition	51 mm Sand-Plaster
Interior Shear-Wall	25 mm Sand-Plaster 102 mm Solid Concrete Block 25 mm Sand-Plaster 38 mm Vented Cavity
Floor Slab	51 mm Wood Floor 203 mm Concrete 25 mm Sand-Plaster
Windows	Frame: Aluminum, Thermally Broken Glazing: Low-Emissivity Double-Glazed

3.1.2 Building Energy Model

This section summarizes how an energy model of the representative building was created. In addition to the reference model, which modeled the “As-Built” building envelope and ventilation systems, several simulated retrofits were also modeled. This section provides the details of the simulated retrofits, including the source and reasoning for key inputs. A more detailed list of model inputs and their sources are summarized in Appendix B.

3.1.2.1 Energy Modeling Overview

16 combinations of retrofits were evaluated in order to determine their impact on how much heating demand can be shifted with variable suite-level temperature control. The retrofit combinations included envelope retrofits, ventilation system retrofits, and various interior finishes. The retrofits to the envelope and ventilation system were based on a recent tower renewal study that presented current best-practices for tower renewals in Canada (Ricketts et al. 2017). The study showed that retrofit measures might be implemented in stages or that only a portion of those measures might be implemented. Thus, the selected retrofit combinations examined the impact of measures individually and in combination.

Table 2 provides a summary of the 16 retrofit combinations modeled for the case study building. 12 versions had a convective heating system, while four had a radiant floor heating system. For the convectively heated models, three had the existing ventilation system and envelope ("Model A-#"); three had an improved envelope ("Model B-#"); three had an improved ventilation system ("Model C-#"); and, three had both the improved envelope and the improved ventilation system ("Model D-#"). For each category denoted by a letter (A, B, C, and D) three interior finishes were considered that exposed or insulated the concrete structure of the building, thereby changing the effects of the building thermal mass. These different combinations of heating systems and interior finishes are denoted by the number in the model names, e.g. "Model D-3".

Table 2 : A Summary of the 16 Retrofit Combinations Modelled in EnergyPlus

Envelope and Ventilation System → / Heating System and Interior Finish ↓		Reference Envelope & Reference Ventilation • Infiltration 0.3 ACH • Pressurized-corridor ventilation 425 L/s	Upgraded Envelope & Reference Ventilation • Add 89mm exterior insulation • ↓ Infilitration to 0.15 ACH • Pressurized-corridor ventilation 425 L/s	Reference Envelope & Upgraded Ventilation • Suite 70% eff. HRV • Infiltration 0.3 ACH • ↓ Pressurized-corridor ventilation to 47 L/s	Upgraded Envelope & Upgraded Ventilation • Both retrofits B & C
Convective Heating	**Reference Finishes** • Wood floor • Slab ceiling w/ plaster coat • Plaster render on block-walls • 51mm sand-plaster partitions	**A-1**	**B-1**	**C-1**	**D-1**
	Exposed Concrete Floor • Exposed concrete floor • Slab ceiling w/ plaster coat • Plaster render on block-walls • 51mm sand-plaster partitions	**A-2**	**B-2**	**C-2**	**D-2**
	Concrete Covered With Lightweight Materials • Rebounded carpet • Acoustic tile ceiling • Gypsum + stud partitions • Gypsum + stud over block-walls	**A-3**	**B-3**	**C-3**	**D-3**
Radiant Floor Heating	**Exposed Concrete Floor** • Exposed concrete floor • Slab ceiling w/ plaster coat • Plaster render on block-walls • 51mm sand-plaster partitions	**A-4**	**B-4**	**C-4**	**D-4**

For models with radiant floor heating, identical combinations of changes to the envelope and ventilation system were considered, but only with the exposed concrete floor finish. This meant that for each radiantly heated model (Row 4), there was a convectively heated model with the same finishes, ventilation system, and envelope (Row 2).

3.1.2.2 Attributes Common to All Models

A typical floor of the building was selected and modeled. This representative floor had a total area of 1263 m^2 and was placed at the mid-height of the building to compensate for height-dependent factors such as shading. Neighboring buildings were modeled to scale as shading elements (Ellis and Torcellini 2005). The exposed slab edges were modeled as a linear transmittance averaged over the remaining surface area, while balconies were modeled as a linear transmittance and a shading element (RDH 2013). The window-to-wall ratio and glazing

properties remained constant, as the windows were recently upgraded to double-glazed low-emissivity units (Touchie 2014).

Estimates of internal loads in the living quarters and common areas were based on a year-long monitoring and calibration study (Touchie 2014), while schedules were obtained from ASHRAE "90.1-2007 Midrise-Apartment" schedule set (ASHRAE 2011). Apartments were assumed to have a nominal lighting load of 6 W/m^2 and a nominal plug-load of 4.8 W/m^2. Hallways were modeled with a constant lighting load of 11 W/m^2 and no plug-loads. Since a lighting retrofit occurred in 2009, further internal-load reductions were not considered. The pressurized-corridor ventilation was modelled as a constant supply of outdoor air pre-heated to 19°C. Recent investigations of pressurized-corridor ventilation in Canadian high-rise residential buildings found that less than 10% of the pressurized-corridor air entered the apartments (Kemp 2013; Ricketts and Straube 2014). Thus, it was assumed that negligible ventilation entered the units.

All models in this study were retrofitted with electric heating systems and variable suite-level temperature control. It was assumed that each unit had suite-level heating system controls, and that all units maintained the same indoor air temperature. Thus, the representative floor was modeled as having a North, South, and hallway zone. This zone configuration was compared to a model with an additional zone for each corner unit. However, the difference in the amount of heating demand that was shifted when corner units were modeled was not significant, so the modelling of corner units was discontinued.

Since load shifting performance has been reported to be sensitive to heating system size (Klein et al. 2017), the heating capacity was sized relative to the heating demand of each model according to ASHRAE energy modeling guidance (ASHRAE 2016). This entailed sizing runs using ASHRAE design day weather files for Toronto and a 25% oversizing factor to obtain the total heating system capacity.

3.1.2.3 Heating System Retrofits

Electric heating systems with both convective heating and radiant floor heating were considered. The radiant floor system represented a case in which the concrete floor slab was directly coupled to the heating system. The convective heating system represented the performance of systems such as baseboard heaters, fan-coils, forced-air, or other similar heating systems which interact

with building thermal mass primarily through changing the temperature of the ambient air and convective coupling between the air and the thermal mass. Although electric heating systems have widely varying efficiencies, the heating systems used in this study were all assumed to have a constant efficiency of 100%, which means that the energy supplied and the heating energy demand were equivalent.

The models with radiant floor heating required a significantly more complex heating system control arrangement than the convectively heated models. For the convectively heated models, the heating system was controlled based on the difference between the indoor air temperature and the setpoint temperature, which is also known as proportional control. For models with radiant floors, two separate heating systems and two independent control methods were required.

The radiant floor models were primarily heated by the radiant floor, but a smaller backup convective heating system was also used. The radiant floor was heated by hot water and the supply temperature of water was calculated based on the outdoor air temperature in order to control the heat output of the floor. Similar to the approach outlined in Olesen (2007), the parameters for the radiant floor temperature control were determined using spreadsheet calculations. The calculations used to determine the heat output of the floor are included in Appendix C, and a sample of the calculations used to determine the control parameters for the radiant floors are detailed in Appendix D.

The radiant floor heating system was very slow to respond and the controls did not account for changes in indoor air temperature. Therefore, with this heating system it was much more difficult to maintain the desired indoor air temperature. To address this issue, a secondary convective system was added in order to maintain the indoor air temperature at a given setpoint. This is a common configuration for radiant floor heating systems in Canada. The small, secondary convective system comprised less than 25% of the total heating capacity for each model, and the combined heating system capacity for models with radiant floor heating was identical to the equivalent convectively heated models. The characteristics of the radiant and the convective heating systems are summarized in Table 3.

Table 3 : HVAC System Parameters Used in Energy Models

Variable	Radiant Floor System	Convective System
Type	LowTemperatureRadiantConstantFlow	Baseboard:RadiantConvective:Electric
Input Variable	Outdoor Air Temperature	Indoor Air Temperature
Output Variable	Water Supply Temperature	Baseboard Power
Hydronic Tubing Spacing	0.152 m	n/a
Radiant Source Layer Type	2-D CTF Calculation	n/a
Internal Source Layer Depth	0.05 m Below Floor Surface	n/a

3.1.2.4 Envelope & Ventilation Retrofits

The infiltration (i.e. unintentional leakage of outdoor air into the building) and ventilation flowrates for each model were based on the characteristics of the envelope and ventilation systems. For the reference envelope and ventilation systems, inputs were based on field work and detailed research (Touchie 2014). In the pre-retrofit cases, a continuous infiltration rate of 0.3 air changes per hour (ACH) was assumed for the apartments in the model, and a continuous infiltration rate of 0.01 ACH was assumed for the hallway. The reference ventilation system supplied ventilation to the hallway at a rate of 425 L/s (900 ft^3/min) per floor, or about 26 L/s (56 ft^3/min) per door.

The upgrade strategies for the ventilation system and envelope were based on a recent deep energy retrofit case study (Ricketts et al. 2017). The upgraded envelope included 89 mm of continuous exterior mineral-wool insulation, and extensive air-tightness measures. A post-retrofit infiltration rate of 0.145 ACH was assumed for the apartments, which was consistent with the post-retrofit air-tightness results for comparable buildings (Ricketts et al. 2013). In the case of

the ventilation retrofit, it was assumed that under-door vents had been sealed and that each floor was compartmentalized, which meant that the hallway ventilation rate could be reduced to 47 L/s (100 ft^3/min) per floor. Additionally, 70% efficient in-suite heat recovery ventilation (HRV) units with a flowrate of 376 L/s (800 ft^3/min) per floor were added in accordance with Canadian residential ventilation standards (CSA 2014). The HRV air supply was modelled as 0.12 ACH of continuous ventilation to the apartments.

3.1.2.5 Interior Finish Retrofits

As seen in Table 2, three interior finish options were considered for the convectively heated models. The exposed concrete floor was the only interior finish option considered for the radiant floor models. The reference finishes consisted of plaster applied to masonry shear-walls, 51 mm thick sand-plaster partitions, wood flooring, and plaster applied to the ceiling slab.

To evaluate the effect of variations in the thermal resistance of floor-slab finishes, two extreme scenarios were considered. In the first case, the wood floor was removed to expose the concrete slab. In the second case, the floor was covered with thick carpeting, the ceiling was covered with a dropped-ceiling of acoustic tiles, and the masonry partition walls were covered with wood-studs and drywall. Covering the slab and partition walls with these materials increased the thermal resistance between the indoor environment and the concrete structure, and thus reduced the thermal mass effect. The composition of building elements and the material properties are summarized in Table 4 and Table 5, respectively.

Table 4 : Composition of the Building Elements Used in Energy Models

Description	Input	Net Area Per Floor (m^2)
Reference Exterior Walls	13mm Gypsum 26mm (E-W wall) or 22mm (N-S wall) EPS* 203mm Concrete**	469
Reference Interior Partition	51 mm Sand-Gypsum Plaster	901
Reference Interior Shear-Wall	25 mm Sand-Gypsum Plaster 102 mm Concrete 25 mm Sand-Gypsum Plaster	688
Reference Floor Slab	51 mm Wood Flooring 203 mm Concrete 13 mm Gypsum	1263
Reference Glazing	Alum. Frame Thermally Broken, Low-E DG (0.42 m^2K/W)	291
Exterior Wall Retrofit	13 mm Gypsum 22 mm EPS 203 mm Concrete (Equivalent Ext. Mass) 89 mm Mineral Fiber Insulation	469
Floor Slab - Exposed Concrete Retrofit	203 mm Concrete 13 mm Gypsum	1263
Floor Slab - Radiant Flooring Retrofit	51 mm Concrete Radiant Layer 203 mm Concrete 13 mm Gypsum	1263
Floor Slab - Lightweight Finish Materials Retrofit	19 mm Rebounded Carpet 203 mm Concrete 13 mm Gypsum Ceiling Air-Gap (0.18 m^2K/W) 19 mm Acoustic Tile	1263
Shear Walls - Lightweight Finish Materials Retrofit	13 mm Gypsum Air-Gap (0.15 m^2K/W) 102 mm Concrete block Air-Gap (0.15 m^2K/W) 13 mm Gypsum	688

* Includes linear-transmittances, and resistance of block.
** Includes mass of concrete block and brick

Table 5 : Material Properties Used in Energy Models

Description	Density (kg/m^3)	k (W/mK)	Cp (J/kgK)
Gypsum Board	785	0.16	830
Sand-Gypsum Plaster	1550	0.65	830
Concrete	2243	1.73	837
Wood Flooring	608	0.15	1630
EPS Insulation	43	0.036	1210
Mineral Fiber Insulation	97	0.042	800
Rebounded Carpet	110	0.045	2500
Acoustic Tile	368	0.06	590

3.1.3 Simulated Building Operation Scenarios

Two scenarios were used to evaluate the building models. In the first scenario, the models were exposed to a typical weather year in Toronto, Ontario. The objective of the full-year scenario was to evaluate how much heating demand could be shifted from peak hours to off-peak hours, and the resulting impacts on GHG emissions and electricity costs.

In the second scenario, the building models were exposed to a few hours of a very cold January evening in Toronto. These hours represent the coldest evenings of the year, as in Ontario those evenings are typically when peak winter electricity demand occurs. The objective of the second scenario was to explore the potential of shifting heating demand in a situation where residential customers are charged for their power draw during the hours of peak electricity demand ($/kW) as well as total energy used ($/kWh). Presently, residential customers in Ontario are charged for their energy usage, but are not charged for their peak power draw. Thus, the exploration of the peak power draw is speculative, but represents how residential users may be charged for electricity in the future.

3.1.3.1 Simulating Shifting Heating Demand in a Typical Weather Year

The models were simulated for a complete year using the Canadian Weather Year for Energy Calculation (CWEC) data for Toronto (Environment Canada 2018). In this scenario, as much heating demand as possible was shifted from hours of the day with expensive and GHG-intensive electricity to hours of the day when electricity was cleaner and cheaper. Further, the load shifting schedules were constrained to maintain an average temperature of 23°C, and to remain within the ASHRAE 55 thermal comfort boundaries (ASHRAE 2017). An optimization approach was not used, and thus the GHG emission and electricity cost savings presented in this research are not necessarily optimal. Rather, a logic-based approach was used to evaluate the impact of shifting heating demand to off-peak hours, while maintaining similar levels of thermal comfort and energy usage (Klein et al. 2017).

Since electricity prices and GHG emissions were generally found to be high at similar times, one heating schedule was developed that avoids both high prices and high GHG emissions. For this schedule, hours were determined to be desirable or undesirable for electricity consumption based on the cost and GHG intensity of electricity. The hourly cost was determined using the current Time-Of-Use electricity prices shown in Figure 4 (Ontario Hydro 2018). The GHG intensity was evaluated using both the Average Emission Factors (AEF) shown in Figure 5, and the Marginal Emission Factors (MEF) shown in Figure 6. AEF and MEF are two methods that have been used by sustainability researchers in Ontario to calculate the GHG emissions associated with electric energy usage (TAF 2017). The AEF were calculated by averaging the total GHG emissions by the total energy usage for the Ontario grid. The MEF were calculated using a more complicated method, which only included certain generation sources.

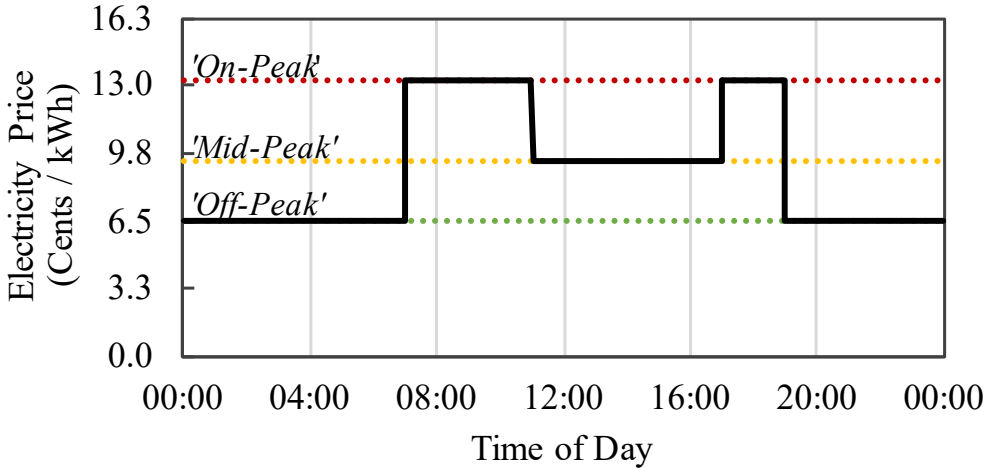

Figure 4 : Time-Of-Use Electricity Prices for Ontario in Winter (Ontario Hydro 2018)

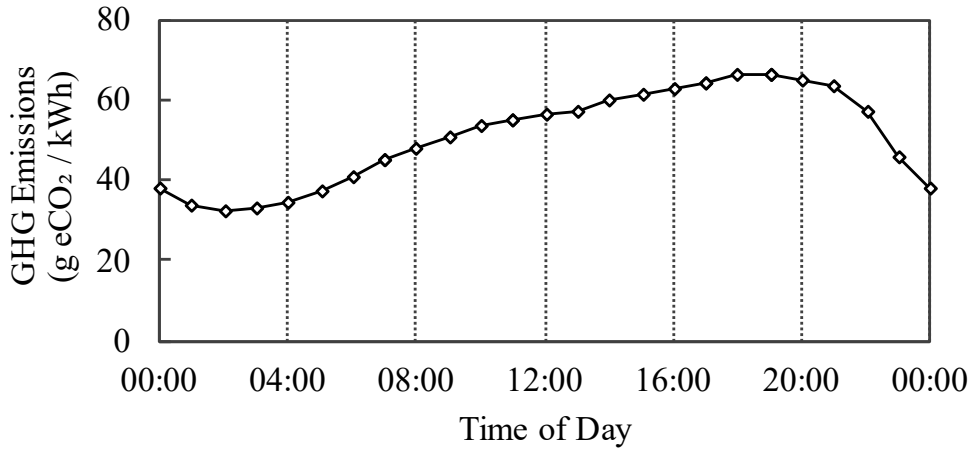

Figure 5 : Average Emission Factors for Electricity in Ontario (TAF 2017)

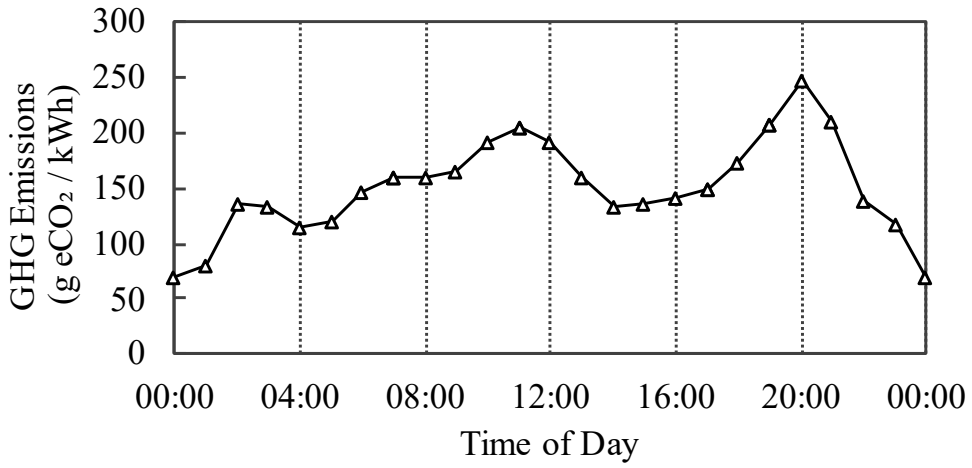

Figure 6 : Marginal Emission Factors for Electricity in Ontario (TAF 2017)

The hourly values for marginal emission factors, average emission factors and electricity prices were divided by their respective daily average, then summed to create a total score for each hour. These scores, provided in Appendix E, were used to sort the hours from most desirable to least desirable for electricity use. It was found that the hours with the eight lowest scores were between 23:00 and 07:00. During these hours, electricity was both less expensive and less GHG intensive than the daily average. Therefore, these eight hours were selected as the charging period. During this period, the thermostat setpoint was increased 2ºC to charge the thermal mass.

Likewise, the eight least desirable hours were determined to occur between 07:00 and 12:00 and between 17:00 and 20:00. During these times, the setpoint was lowered by 2°C to discharge the thermal mass thereby reducing heating demand. For the remaining eight hours, the setpoint was left neutral at 23°C. Since the hours above and below 23ºC were equal, the average setpoint temperature remained 23ºC. If the indoor temperature followed the setpoint closely, the average air temperature was close to 23°C and the energy use was similar to an identical model operated at a 23ºC setpoint.

Figure 7 shows the default schedule created using this process, and the resultant net energy usage relative to an identical model operated at 23ºC.

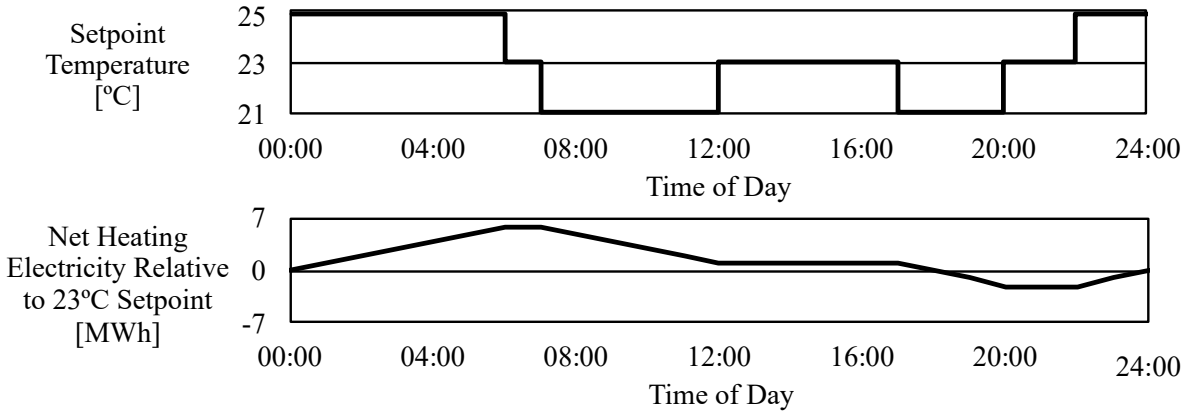

Figure 7 : Default Load Shifting Thermostat Schedule, and the Net Heating Electricity Usage Relative to Operating at 23ºC

When the heating system was required to run continually, as is the case in cold weather, the indoor temperature remained close to the setpoint. However, when the outdoor temperature was warmer, the thermal mass often met the whole heating requirement. In this case, the interior air temperature slowly drifted downwards after a setpoint reduction. When the default schedule was used, this slow downward drift resulted in an average temperature greater than 23°C. Figure 8 shows the process by which the default schedule was modified if it was necessary to reduce the average indoor air temperature due to warmer weather. To reduce the average indoor air temperature, neutral hours were added to the discharging period. The eight least desirable hours for electricity use were already part of the discharging period and the setpoint could not be lowered further without compromising thermal comfort. Thus, starting with the ninth least desirable hour, the setpoint was reduced from 23°C to 21°C. If overheating persisted, the next least desirable hour was added to the discharging period until the average temperature and energy usage matched the same model operated at 23°C. By lowering the setpoint in neutral hours rather than reducing the number of thermal mass charging hours, the amount of heating demand shifted to off-peak hours was maintained or increased whenever possible.

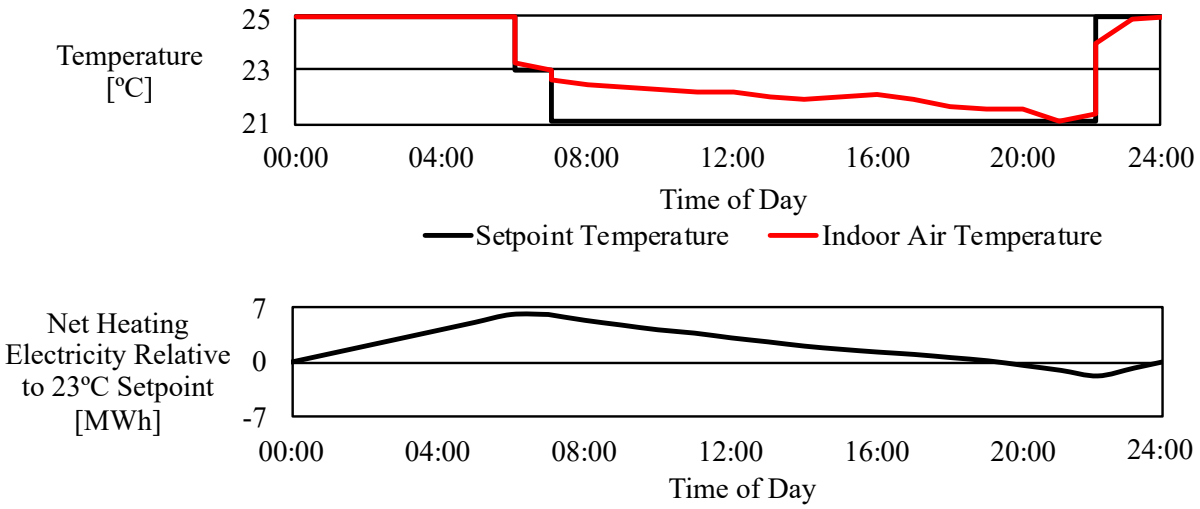

Figure 8 : Typical Load Shifting Thermostat Schedule and Indoor Air Temperature Response during Moderate Weather; and the Net Heating Electricity Usage Relative to Operating at 23ºC

The same method was applied to the models with radiant floor heating. However, the indoor air temperature was only varied between 22°C and 24°C for models with radiant floors. Since, for radiant floors, the thermal mass is directly coupled to the heating system, thermal energy can be transferred into the slab very effectively without increasing the indoor air temperature. Further, the slab temperature can be increased above room temperature to enhance heat transfer from the slab to the room. Thus, the smaller indoor air temperature range was sufficient to achieve equivalent load shifting performance to radiantly heated models for which the indoor air temperature was varied between 21ºC and 25ºC.

3.1.3.2 Evaluating Electricity Cost and GHG Savings in Ontario

The GHG emissions and heating costs for models in the full-year simulation were evaluated using current Ontario electricity prices and GHG emissions data. As previously mentioned, and shown in Figure 4, electricity costs were calculated using winter Time-Of-Use electricity prices. In the initial analysis, MEF and AEF were both used to calculate GHG emissions. The hourly AEF and MEF for Ontario were previously shown in Figure 5 and Figure 6, respectively. A detailed description and a sample of these calculations are provided in Appendix F and Appendix G, respectively.

To calculate heating costs and GHG emissions, a heating system efficiency of 100% was assumed, which is equivalent to electric resistance heating. However, the results may be scaled to represent other heating systems for which the heating efficiency can be easily estimated, such as ground-source heat pumps. For other types of systems where the efficiency has strong seasonal or diurnal variations, such as air-source heat pumps, charging at night might be significantly less efficient. Thus, further calculations that were not carried out here would be required to determine the resulting GHG emission and heating cost savings.

For this research, electricity cost and GHG emission savings for each model were calculated relative to a "baseline" model. For each model, the baseline model was identical in all ways except that it was operated with a different thermostat schedule. Unlike the models for which the thermostat setpoint was varied frequently in order to shift heating demand, the baseline models were always operated at a 23ºC setpoint in order to avoid shifting heating demand. Thus, in this comparison, thermal comfort conditions were not necessarily the same. However, the average daily temperature was equal in all models and all of the models were operated within accepted winter thermal comfort boundaries, as outlined in the ASHRAE thermal comfort standard (ASHRAE 2017). The rate of temperature change was also considered. Research suggests that occupants find temperature changes within the comfort zone acceptable up to a rate of 4°C / hour (Toftum et al. 2008; Olesen 2012). Thus, for the models compared, the levels of thermal comfort were similar, and the annual heating energy usage was the same within ± 0.5%.

3.1.3.3 Shifting Heating Demand During the Peak Winter Electricity Demand Scenario

In many places, including Ontario, large industrial and commercial electricity consumers are charged for their peak power draw ($/kW) as well as their energy usage ($/kWh). Residential customers in Ontario are not currently charged for their peak power draw. However, that may change soon as the introduction of technologies such as electric cars and distributed photovoltaic generation mean that some residential customers will impose a disproportionate demand on the grid infrastructure. Some customers might use very little energy (kWh) but have a very large peak demand (kW), whereas the opposite might be true of others, so it is unfair to charge all people an equal amount for grid construction and maintenance. Demand charges are being considered and tested by electricity providers in North America to better align the costs of

supplying electricity to each residential customer with how much each customer is charged (Hledik 2014).

Ontario has made several moves towards more widespread application of demand charges. These included incrementally reducing the minimum participant size for pricing structures with demand charges over a period of years (IESO 2019a) and running several small trials that gave residential users smart-thermostats that respond to summer time peak electricity demand (Wong et al. 2017).

In this research, a scenario was explored wherein residential customers were charged for their peak power draw in order to examine the effectiveness of varying the thermostat setpoint to reduce demand charges. However, there is not a common formula for residential demand charges in North America. Rather, the method of applying demand charges and the proportions of demand charges ($/kW) to energy charges ($/kWh) vary to suit the needs of the utility provider (Hledik 2014). In Ontario, large industrial and commercial electricity customers that enroll in the "Class-A" program are charged for both their peak electricity demand as well as their total energy usage. Since the price structure for Class-A customers is indicative of the needs of electricity providers in Ontario, in this research it was assumed that a pricing structure identical to that of the Class-A program would be offered to residential users in the future.

In the Class-A program, demand charges are based on a user's electricity power draw during the five hours of the year when the electrical grid is under greatest load. These hours are commonly known as the "demand peaks". In order to determine how effectively load shifting might be used to reduce these demand charges, models were exposed to a simulated peak winter electricity demand scenario. The peak winter electricity demand scenario used data for January 27th in the typical weather year for Toronto (Environment Canada 2018). January 27th is the coldest day of the typical weather year for Toronto and represents typical conditions during recent winter electricity demand peaks (IESO 2019b). It was assumed that the electrical demand peak began at 5pm. It was also assumed that the building was operated at 23°C for the rest of the winter, and that occupants would be comfortable at temperatures between 21°C and 25°C.

Figure 9 shows the three load shifting strategies that were tested for each model in the peak winter demand scenario. In the "Simple Setback" strategy, the thermostat setpoint was reduced from 23°C to 21°C at 5 PM on the day of the peak. Since grid operators in Ontario typically

indicate that a peak is approaching several hours in advance, two “pre-charge” strategies were also tested. In the pre-charge strategies, the thermostat was set to 25°C for four or twelve hours in advance of the peak, then reduced to 21°C at the beginning of the demand peak.

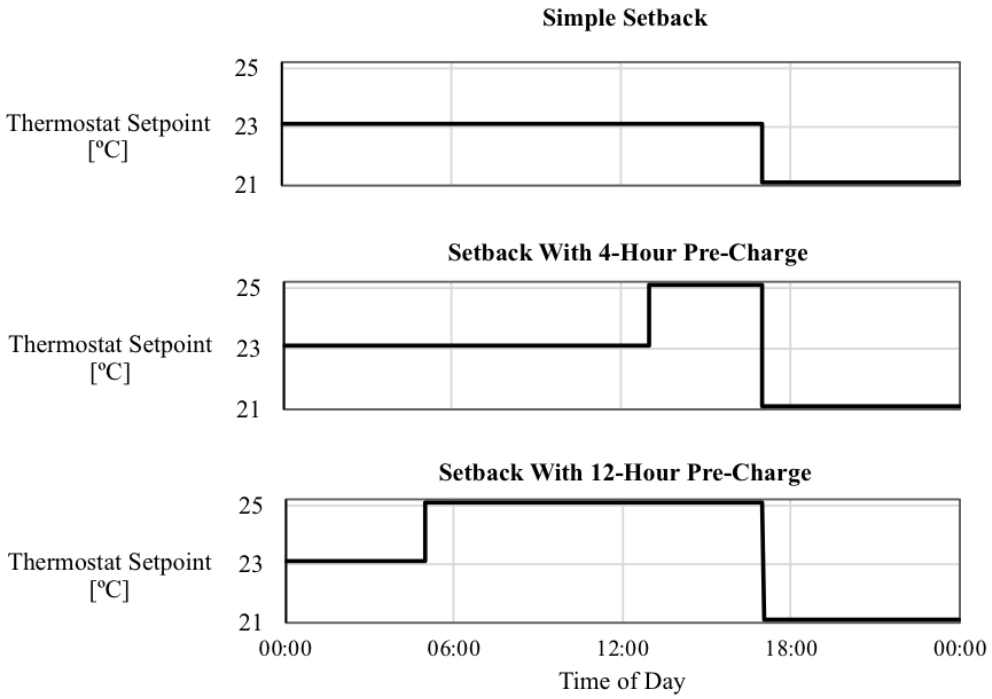

Figure 9 : The Three Thermostat Schedules Used to Shift Heating Demand in the Peak Winter Demand Scenario

3.1.3.4 Evaluating Financial Implications of Electricity Demand Charges

As indicated, since residential electricity customers in Ontario are not currently charged for their power demand ($/kW), the Class-A pricing structure for large industrial and commercial customers was used to examine the financial implications of using variable suite-level temperature control and load shifting to avoid demand charges (IESO 2019a). Class-A customers pay demand charges based on their electricity demand (kW) during the five hours of the year when the Ontario electrical grid is under the greatest load, and also pay for their electric energy usage (kWh) at the real-time market prices known as Hourly Ontario Electricity Prices (HOEP). Unlike Time-Of-Use hourly prices which follow a pre-determined schedule, HOEP prices vary throughout the day and throughout the year based on the constantly changing market price.

An averaging approach was used to estimate the financial impacts of being charged the HOEP prices. Since the savings attained with load shifting are proportional to the variability in electricity prices, the impact of the greater variability in HOEP relative to Time-Of-Use prices was estimated by scaling the savings that were attained using the Ontario Time-Of-Use prices. It was assumed that for each electricity pricing structure, the percentage savings from load shifting were proportional to the ratio of electricity prices during the eight most expensive hours to electricity prices during the eight least expensive hours each day. In 2018, this price ratio was 1.9 for the Time-Of-Use prices and 4.6 for HOEP (IESO 2019c). The scaled savings percentage was then applied to the heating energy cost (kWh), which was calculated with HOEP pricing for each model at 23°C.

For the Class-A price structure, monthly demand charges are calculated based on a customer's energy usage during the five hours each year when the electrical grid is under the greatest load. During the past five years, 20% of these peak electricity demand hours in Ontario have occurred during the winter. Therefore, the calculations assumed that one event occurs in the winter and four occur in the summer. Just as January 27th of the CWEC year for Toronto is typical of conditions for recent winter electricity demand peak, July 8th of the CWEC Year for Toronto is typical of recent summer demand peak conditions (IESO 2019b).

The building electrical demand used in calculating demand charges included electric heating, plug-loads, lighting, ventilation equipment and air-conditioning. The annual demand during the five peak hours was then used to determine monthly demand charges ($/kW) according to the standard Class-A formulae (IESO 2019a).

3.2 Results & Discussion

Results are presented for the models in two scenarios: The typical year scenario, and the winter demand peak scenario. The typical year scenario estimates the financial savings and GHG emission reductions that are currently possible using variable suite-level temperature control to shift heating demand. The winter demand peak scenario is speculative and estimates how much money users would save by shifting heating demand if residential customers were charged for their peak power usage at the same rate that Class-A commercial and industrial users are charged today. This section contains a selection of the results. Additional results are included in Appendix H.

3.2.1 Simulating Shifting Heating Demand During the Typical Year Scenario

This section explores the relationship between various building characteristics and how much heating demand could be shifted in order to reduce electricity costs and GHG emissions during a simulation of a typical year in Toronto. A variety of retrofits to the model building were simulated and for each model variant the reduction in electricity costs and GHG emissions were estimated using current GHG emission factors and Time-Of-Use electricity prices. Figure 10 shows the annual heating energy usage between the hours of 07:00 and 23:00. The remaining hours of the day, between 23:00 and 07:00, were previously determined to be the most desirable hours of the day for electricity use and were designated to be the charging period. In the ideal case, heating electricity would only be used during the charging period. The numbers in red indicate what percentage of heating energy use was shifted to the charging period, relative to the same model operated at a constant 23ºC setpoint.

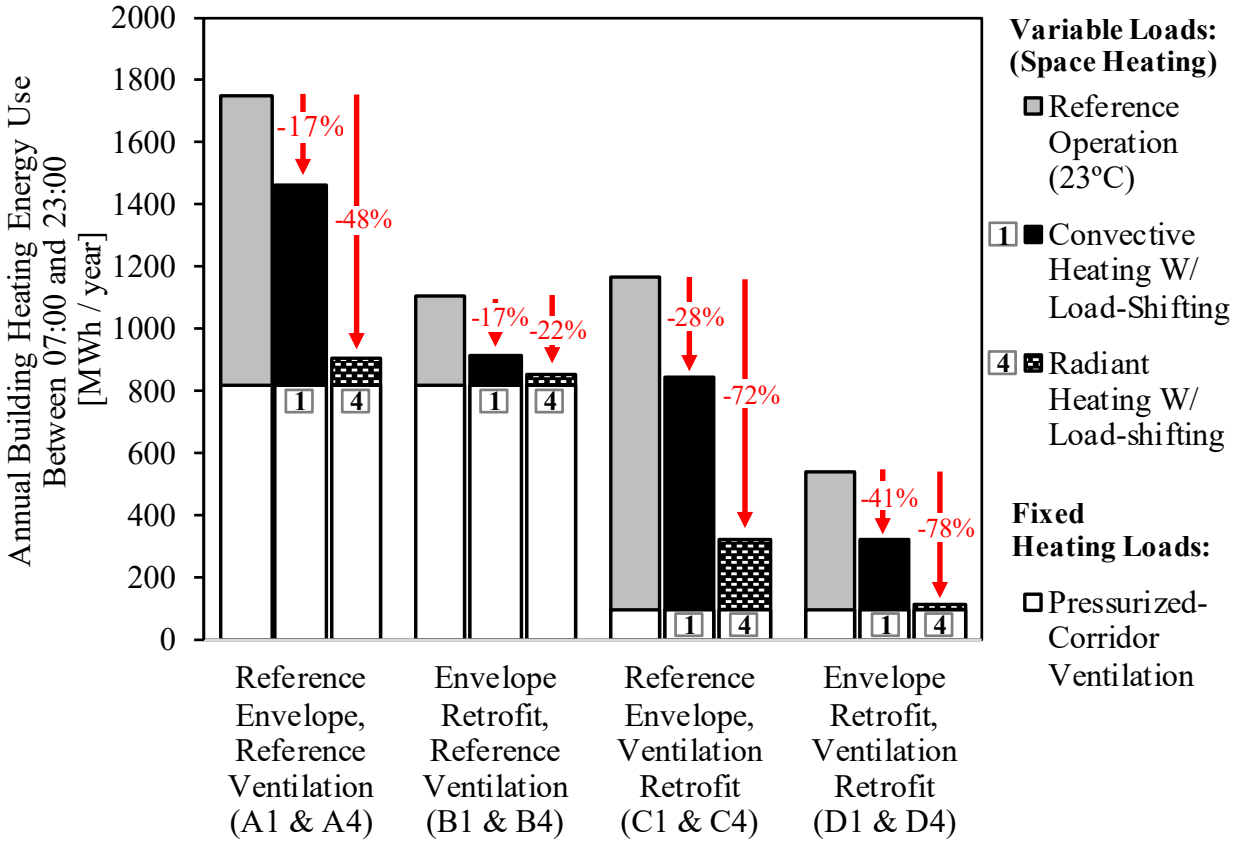

Figure 10 : The Effect of Load Shifting on the Annual Heating Energy Usage Between 07:00 and 23:00 by Heating System Type and Building Retrofit

3.2.1.1 Most Influential Variables: The Building Envelope and the Type of Heating System

As shown in Figure 10, retrofits of the building envelope and ventilation systems both resulted in significant reductions in annual heating energy usage. However, with respect to the amount of heating demand that could be shifted, the building envelope retrofit was found to have a greater effect. To understand the influence of these parameters, it is necessary to understand the difference between space heating and pressurized-corridor ventilation heating with respect to shifting heating demand.

In Figure 10, the annual heating energy usage between 07:00 and 23:00 is divided into the energy used for space heating (i.e. heating of the apartments), and the energy used for heating of

the pressurized-corridor ventilation. The amount of energy used for space heating was primarily determined by the building envelope, since heat loss from the apartments was primarily due to infiltration and conduction through windows and walls. When the thermostat setpoint in the apartments was reduced, heat flowed from the thermal mass, and reduced the need for additional space heating. Since the space heating energy usage was significantly changed by varying the thermostat setpoint, the space heating energy usage is said to be "variable" with respect to shifting heating demand.

Conversely, the energy used for heating the pressurized-corridor ventilation was found to be "fixed" with respect to shifting heating demand. The pressurized-corridor ventilation system was assumed to run constantly to ensure adequate indoor air quality and to provide fire safety. Further, as described previously in Section 3.1.2.2, the pressurized-corridor ventilation was assumed to escape the building without entering the apartments, and thus was not related to space heating energy usage. As a result, changing the thermostat setpoint in the apartments did not significantly affect the energy usage for heating the pressurized-corridor ventilation.

As shown in Figure 10, although reducing the pressurized-corridor ventilation airflow greatly reduced the annual heating energy usage, it had no effect on the amount of heating demand that could be shifted. However, as part of the ventilation retrofit, suite-level HRV units were also added. These HRV units placed an additional load on space heating systems. Thus, the main effect of the ventilation retrofit was to slightly increase the amount of heating demand that could be shifted by varying the thermostat setpoint. In the case of the building envelope retrofits, improving the envelope greatly decreased the space heating demand, and the amount of heating demand that could be shifted was proportionally reduced. Thus, changes to the building envelope were much more influential than changes to the ventilation system with respect to the amount of heating demand that could be shifted.

The type of heating system also significantly influenced the amount of heating demand that was shifted. More heating demand was shifted if models had radiant floor heating. Thermal energy can be transferred much more quickly into the floor slab with a radiant floor system, as the heating system and the thermal mass are directly coupled. Convective systems are limited by the rate of heat transfer between the indoor air and the thermal mass. As seen in Figure 10, the

superior heat transfer of radiant floors had a greater effect for models with greater space heating demand.

3.2.1.2 Least Influential Variable: Interior Finishes

Figure 11 further illustrates the net reduction in annual heating energy usage between 07:00 and 23:00 achieved with load shifting for models with radiant floor heating, and for models with convective heating and various interior finish retrofits. The reduction for each model is relative to the same model operated with a constant setpoint temperature of 23ºC.

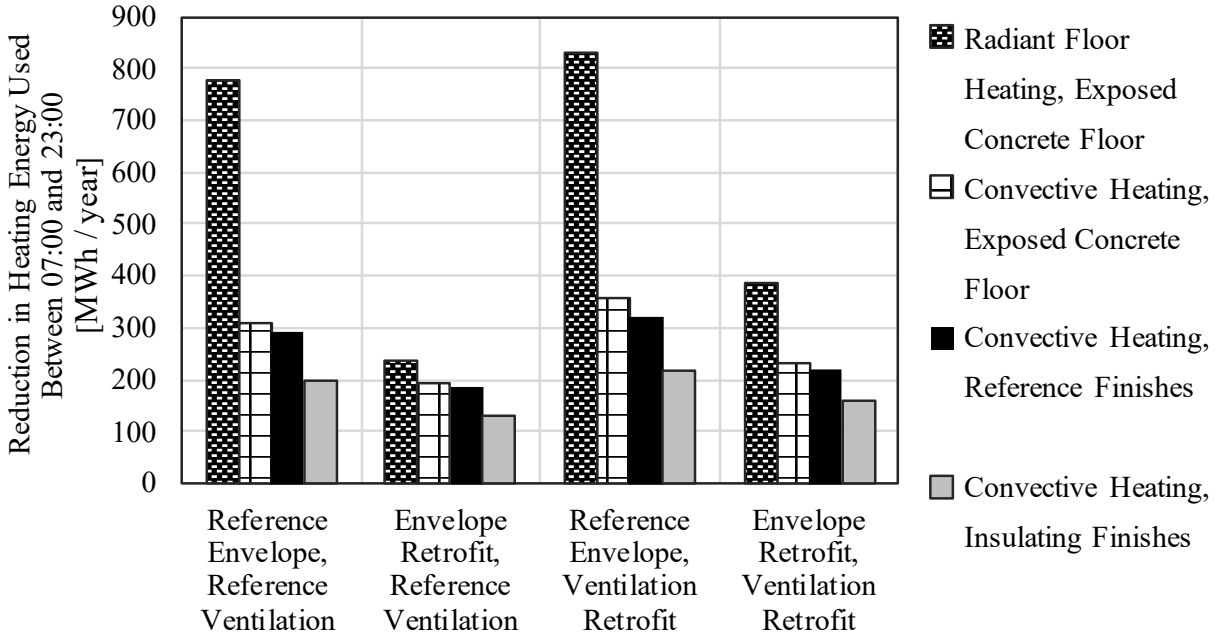

Figure 11 : The Net Reduction in Annual Heating Energy Usage Between 07:00 and 23:00 Using Load Shifting for 16 Retrofit Combinations *

*Relative to an identical model at 23°C

As seen in Figure 11, for the typical year simulation the effects of changing the interior finishes on load shifting performance were less significant than the effects of changing the envelope, changing the ventilation system, or changing the heating system. For the convectively heated models with insulating finishes, the concrete slab was covered with rebounded carpet (R-0.42 m^2K/W) and acoustic-tile assemblies (R-0.47 m^2K/W). Due to the insulating finishes, the amount of heating demand shifted by thermal mass was reduced by up to 30% compared to an equivalent

model with the reference interior surface finishes. Figure 11 also shows that the results for models with an exposed concrete floor differed from the results for models with the reference finishes by less than 10%. Since the difference in performance between the reference finishes and the exposed concrete floor was relatively small for the cases considered, the results for convectively heated models with the exposed concrete floors are not shown in other figures.

3.2.1.3 The Electricity Cost and Greenhouse Gas Emission Savings in Ontario

In order to determine the impacts of using MEF or AEF, both sets of emission factors were used to calculate the GHG emissions for each model. Figure 12 shows the percentage reduction in GHG calculated twice for every model run: once with MEF and once with AEF (TAF 2017). The percentage reduction in GHG emissions for each model was calculated relative to the same model operated at 23ºC. It was found the GHG emission savings determined with the Ontario MEF and AEF were quite different in terms of magnitude (Tonnes eCO_2), but quite similar in terms of percentage benefit. Thus, the results were not greatly skewed by using either factor. Rather, in the cases considered, using the AEF consistently resulted in a more conservative estimate of the reduction in GHG emissions.

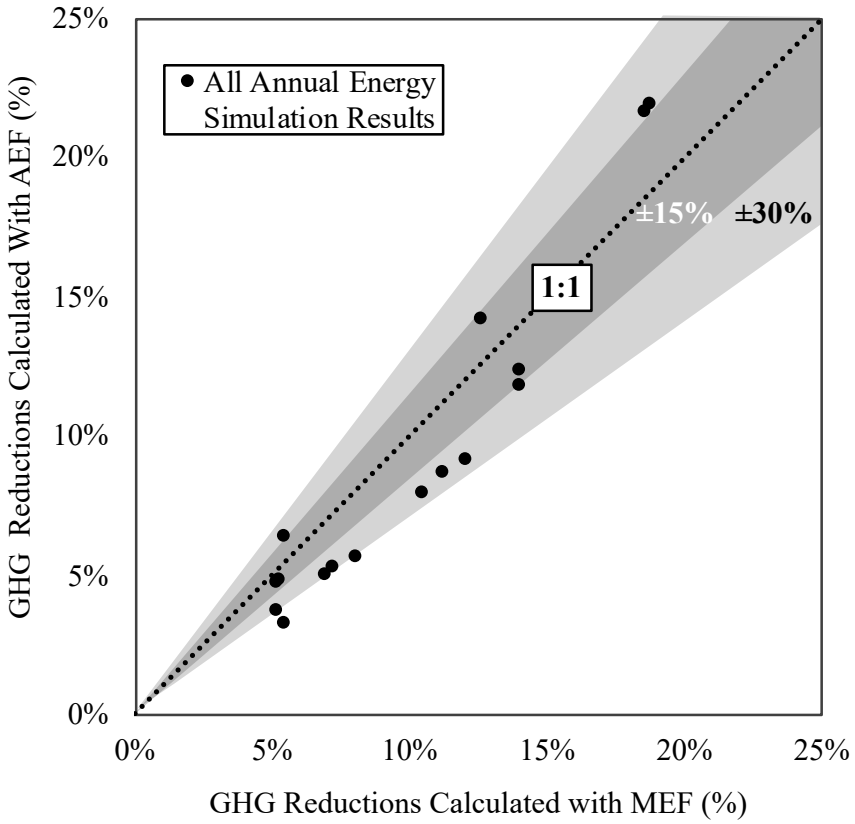

Figure 12 : Percentage Reduction in Annual Greenhouse Gas (GHG) Emissions Using Load Shifting for 16 Models as Calculated Using Marginal Emission Factors (MEF) and Average Emission Factors (AEF)*

*Relative to an identical model operated at 23ºC.

The more significant difference between the MEF and AEF for Ontario electricity was the complexity of the calculations used to create each set of emissions factors. The calculations used to create the MEF were significantly more complex than calculations for the AEF, and required significantly more assumptions (Farhat and Ugursal 2010; TAF 2017). Further, there are actually many accepted ways to calculate MEF, but the results of these calculations vary widely (Ryan et al. 2016). Given that AEF are generally simpler and more standardized than MEF, and that the AEF available for Ontario resulted in more conservative estimates of GHG reductions than the MEF available for Ontario, AEF were used for the remainder of this analysis.

Figure 13 shows the annual GHG savings achieved for the 300-unit models by varying the thermostat setpoint, as calculated using AEF. Similar to Figure 11, the GHG savings for each model in Figure 13 are relative to the same model operated at 23°C. By assuming a heating system efficiency of 100%, the annual GHG savings were found to be between 4 Tonnes eCO_2 and 7 Tonnes eCO_2 for convectively heated models and between 6 Tonnes eCO_2 and 20 Tonnes eCO_2 for models with radiant floor heating. This quantity of GHG is approximately equal to the GHG emitted annually by 2 to 4 cars (US EPA 2018), or by 3 to 5 Canadian homes heated with natural gas (Statistics Canada 2008). If these emissions were to be offset by purchasing carbon offsets online, avoiding 20 Tonnes eCO_2 would cost $640 (Less 2019). The fact that the reductions were found to be quite modest reflects the generally low GHG intensity of electricity generation in Ontario. As shown previously in Figure 5, the difference in GHG intensity during peak and off-peak hours was quite small. If that difference had been greater, the reduction in GHG would also have been greater.

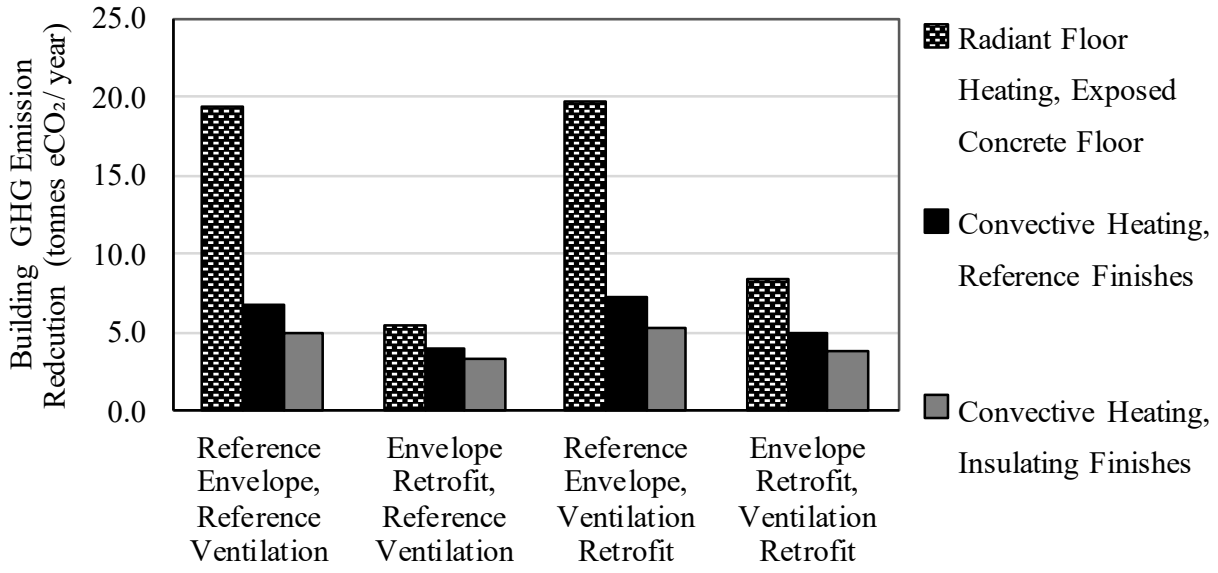

Figure 13 : The Annual Greenhouse Gas Emission (GHG) Savings using Load Shifting and Average Emission Factors for Various Building Retrofits*

*For a 300-unit building relative to the same model operated at 23°C, and assuming a heating system efficiency of 100%

Figure 14 shows the annual reduction in heating electricity costs for a 300-unit building model relative to an identical model operated at a setpoint of 23ºC throughout the heating season. Assuming a heating system efficiency of 100%, and using current Ontario Time-Of-Use prices, the reduction in annual electricity cost savings were found to be between $8,000 to $18,000 for convectively heated models and between $10,000 to $34,000 for models with radiant floor heating. The results in Figure 14 reveal trends similar to those shown in Figure 13. However, in every case electricity cost savings were at least ten times greater than the $640 market value of avoiding 20 Tonnes eCO_2. Thus, given the current grid characteristics in Ontario, the electricity cost savings from shifting heating demand were found to be more substantial than the reduction in GHG.

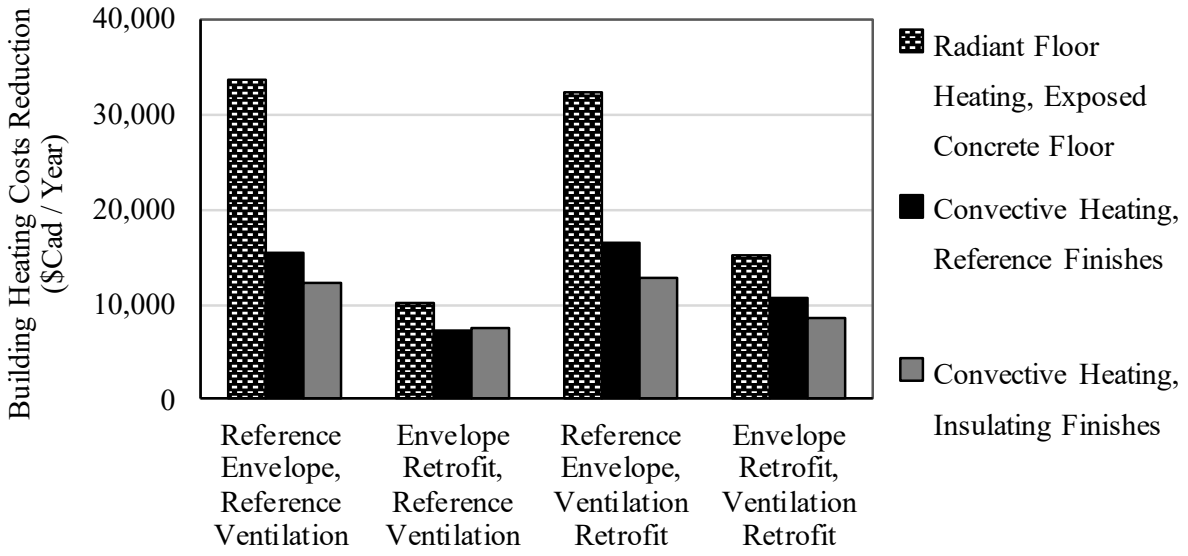

Figure 14 : The Annual Electricity Cost Savings using Load Shifting and Time-of-Use Electricity Prices for Various Building Retrofits

*For a 300-unit building, relative to same model at 23°C, and assuming a heating system efficiency of 100%

3.2.2 Simulating Shifting Heating Demand During the Peak Winter Electricity Demand Scenario

The peak winter electricity demand scenario was used to estimate the electricity cost savings possible in a situation where residential customers are charged for both their electric energy usage and their peak electric power demand. Residential customers in Ontario are not currently charged for their peak power demand. However, as has been mentioned, many electricity providers are considering demand charges for residential customers as these charges would more fairly charge consumers for technologies that place a disproportionate demand on the grid, such as electric vehicles.

In this research, the existing electricity price structure for large industrial and commercial Class-A customers in Ontario was used to explore the potential of using variable suite-level temperature control to shift heating demand in high-rise residential buildings. Demand charges for Class-A customers are based on their electricity demand during the five hours of the year when the electrical grid is under the greatest load. To evaluate how demand charges could be reduced by shifting heating demand, for each model the thermostat was set back during a

simulated winter electricity demand peak. Additionally, convectively heated models were pre-charged by setting the thermostat to 25°C for either four or twelve hours in advance of the winter electricity demand peak, then set back to 21ºC at the beginning of the peak. These strategies were shown previously in Figure 9.

Figure 15 shows the typical response for radiant and convective heating systems after the thermostat setpoints were reduced. “Hour 0” corresponds to the start of the simulated winter electricity demand peak. After the thermostat was set back at hour 0, heating demand was reduced due to the contribution of the thermal mass to space heating. As seen in Figure 15, for models with radiant floor heating, after reducing the thermostat setpoint 1ºC, no additional energy was required for space heating demand for six hours. However, the heating demand did not go to zero as heating energy was still required for the pressurized-corridor ventilation system. For convectively heated models, the heating demand was reduced but remained greater than for radiantly heated models, and gradually increased over the six hours.

The reduction in heating demand used to calculate electricity cost savings was the difference between the heating demand of a model which had a reduced thermostat setpoint, and the heating demand of the same model operated at 23ºC. To be conservative, the difference in heating demand four hours after the setback was chosen as the typical heating demand reduction.

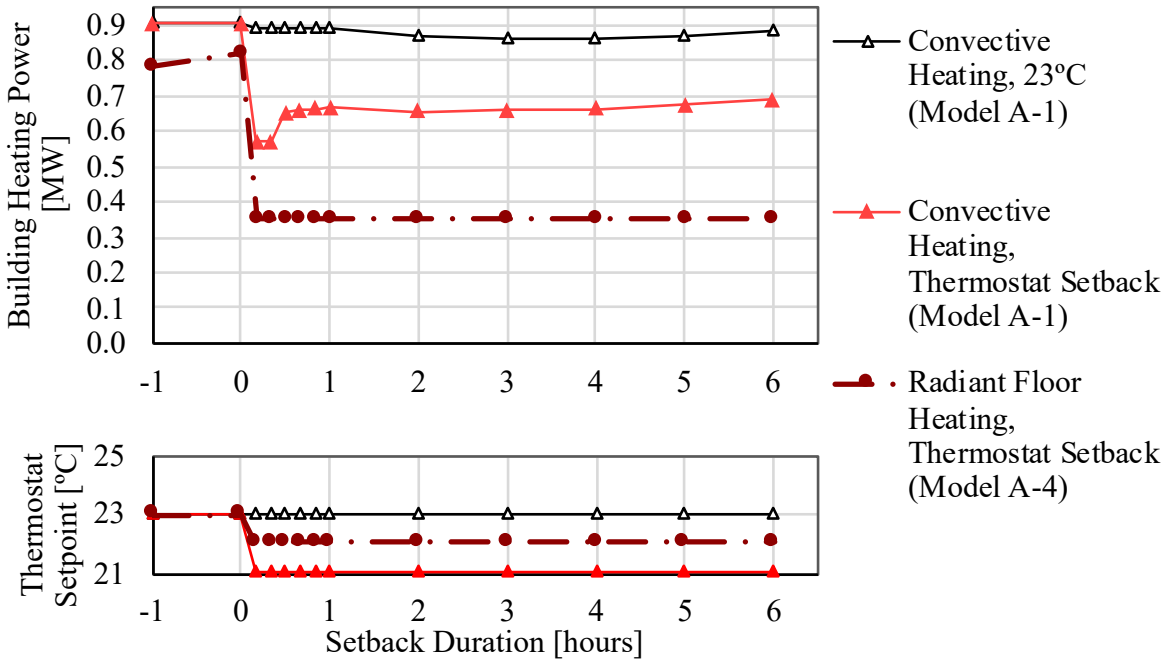

Figure 15 : The Effect of a Thermostat Setback on Simulated Heating Demand during the Peak Winter Demand Scenario for Models with Convective and Radiant Heating Systems

Figure 16 shows the reduction in heating demand four hours after the thermostat setback, relative to an identical model operated at 23ºC. Whereas Figure 15 only shows the results for models which simply had their setpoints reduced, Figure 16 also shows the results for convectively heated models that were pre-charged. For all models with radiant floor heating, space heating demand was still eliminated four hours after the thermostat setback. Therefore, pre-charging was not studied for models with radiant floor heating.

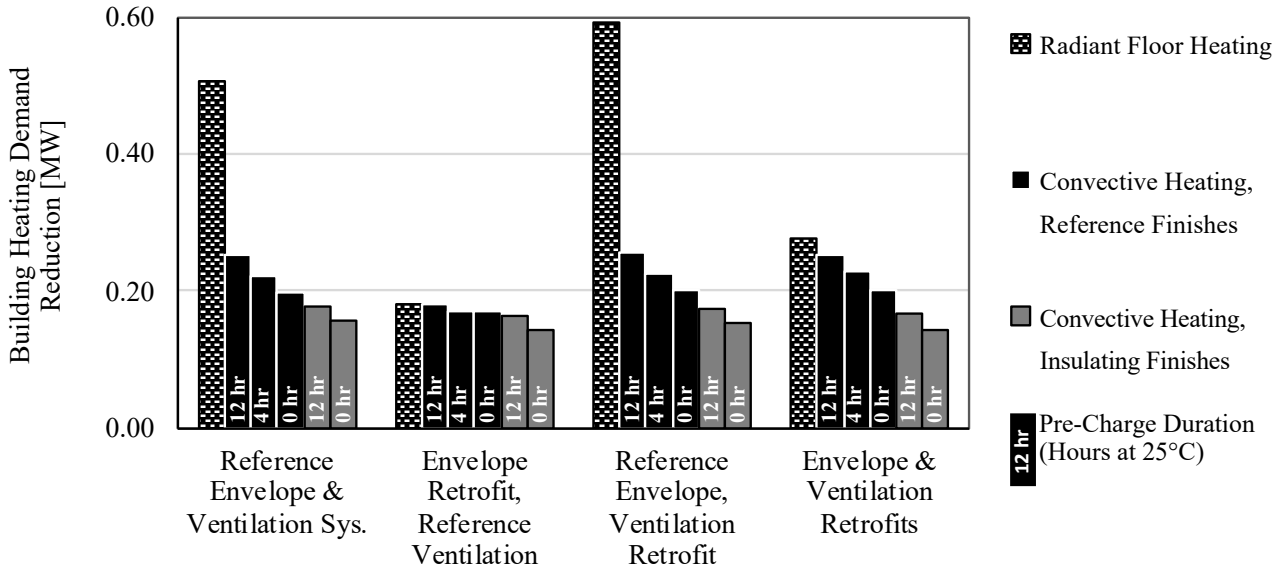

Figure 16 : The Reduction in Peak Winter Heating Demand by Building Retrofit and Pre-Charging Duration*

*For a 300-unit building four hours after thermostat setback, relative to an identical model at 23°C

3.2.2.1 Most Influential Variables: Heating System Type and Pre-Charging

Figure 16 shows that during the peak winter electricity demand scenario, the type of heating system and the use of pre-charging had the largest effect on how much heating demand could be shifted. The results shown in Figure 16 are similar to the results for shifting heating demand during the typical weather year, shown previously in Figure 11, in that radiant floor heating was of the greatest benefit for the models with large space heating demand, and was less beneficial for models with low space heating demand.

Figure 16 also shows that pre-charging was an effective strategy for improving the performance of convectively heated models. Consider a comparison of convectively heated models that were pre-charged for 12 hours, to the convectively heated models that were not pre-charged. With pre-charging, up to 20 kW more heating demand was shifted for models with insulating finishes, and up to 50 kW more heating demand was shifted for models with the reference finishes. Thus, compared to the insulating finishes, the reference finishes were found to enhance the effect of pre-charging. Further, the combination of reference finishes and 12 hours of pre-charging

resulted in up to a 90 kW, or 65%, greater reduction in heating demand than the equivalent model with insulating finishes and no pre-charging.

3.2.2.2 Key Difference: The Influence of the Building Envelope

One key difference between the results for the winter peak demand scenario and the results for the typical year scenario was the effect of the building envelope on the performance of convectively heated models. Figure 11 shows for the full-year simulation, the building envelope was one of the most influential variables for convectively heated models. Conversely, Figure 16 shows that for the peak winter electricity demand scenario, changing the building envelope had almost no impact on how much heating demand could be shifted for convectively heated models. This was due to the greater heating requirements during the peak winter electricity demand scenario. For convectively heated models, in each case the heating requirement was greater than the heating power that could be supplied by the thermal mass. As a result, for each convectively heated model, a similar amount of heating demand was shifted.

As seen in Figure 16, the amount of heating demand shifted was highly variable for models with radiant floor heating. For models with radiant floor heating, the temperature of the thermal mass was controlled to meet the greater heating requirement during the extremely cold weather. This meant the concrete slab temperature was higher in poorly insulated building models, as required to maintain the indoor air temperature at the setpoint. Hence, for models with radiant floor heating the initial temperature of the thermal mass was higher for models with greater space heating demands, and greater amounts of heating demand could be shifted. Thus, for radiantly heated models, the amount of heating demand shifted was still impacted by the building envelope.

The results for models with convective heating are inconsistent with the relatively common assumption that more energy-efficient buildings will not shift great amounts of heating demand (Le Dréau and Heiselberg 2016). While this conclusion may be true at more moderate temperatures, since winter electricity demand peaks in Ontario often occur during extremely cold weather, significant demand shifts may be achieved in energy-efficient, as well as less energy-efficient, buildings.

3.2.2.3 Electricity Cost Savings when Charged Class-A Prices

The financial implications of using load shifting to avoid electricity demand charges were evaluated using the Ontario Class-A electricity prices. The Class-A price structure is currently used for large commercial and industrial users in Ontario and includes a demand (power) charge ($/kW) as well as an energy usage ($/kWh) component. Thus, the financial implications were influenced both by how much energy could be shifted in the typical year scenario, and how much heating demand could be shifted during the peak winter demand scenario. Figure 17 shows the annual heating electricity cost savings achieved with load shifting when Class-A electricity rates were used, compared to the same model operated at 23ºC. These cost savings are displayed as a percentage of total heating electricity costs in Appendix H.

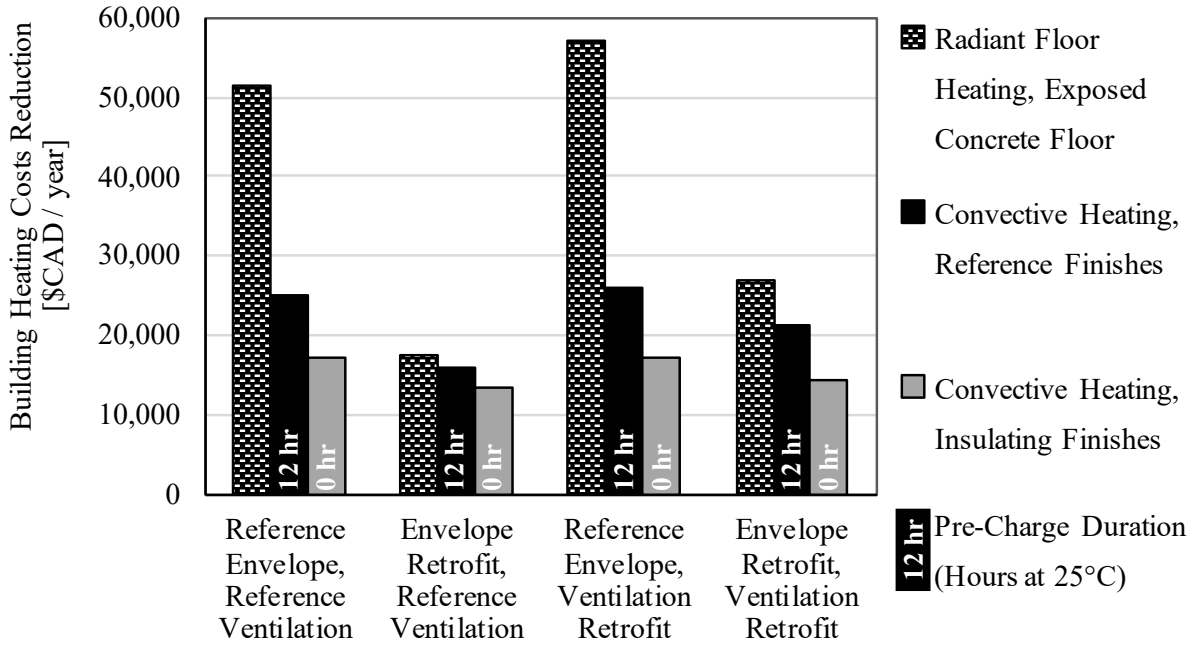

Figure 17 : The Annual Heating Cost Savings Using Load Shifting and Class-A Electricity Prices for the Most Differentiated Combinations of Retrofits and Pre-Charging Durations*

*For a 300-unit building relative to an identical building operated at a 23°C setpoint, and assuming a heating system efficiency of 100%

Comparing the electricity cost savings presented using Class-A prices, as seen in Figure 17, to those cost savings using Time-of-Use prices, as shown previously in Figure 14, the general

trends in electricity cost savings appear quite similar. However, in the case of Class-A electricity prices, the electricity cost savings were significantly greater.

Although the calculations assumed one electricity demand peak occurred in the winter and four occurred in the summer, the electricity demand of each model during the single peak winter demand event was two to six times greater than during each peak summer demand event. Thus, shifting heating demand during the one winter demand peak was still effective at reducing demand charges. By varying the thermostat setpoint during the one winter demand peak, demand charges were reduced by between 9% and 12% for convectively heated models and between 9% and 29% for models with radiant floor heating. It should be noted that these calculations assumed a heating system efficiency of 100%. For a more efficient heating system, shifting heating demand would not have as strong an influence on demand charges. However, given that winter demand peaks occur during particularly cold weather, air-source heat pump systems would be operating much less efficiently than at more moderate temperatures and could well be relying on electric resistance backup heating.

As shown in Figure 17, the greatest savings were obtained for the two models with the poorly insulated reference envelope and radiant floor heating. While keeping the indoor air temperature between 22°C and 24°C, the annual heating costs for each model were reduced by over $50,000.

3.2.3 Key Results for Load Shifting Using Variable Suite-Level Temperature Control

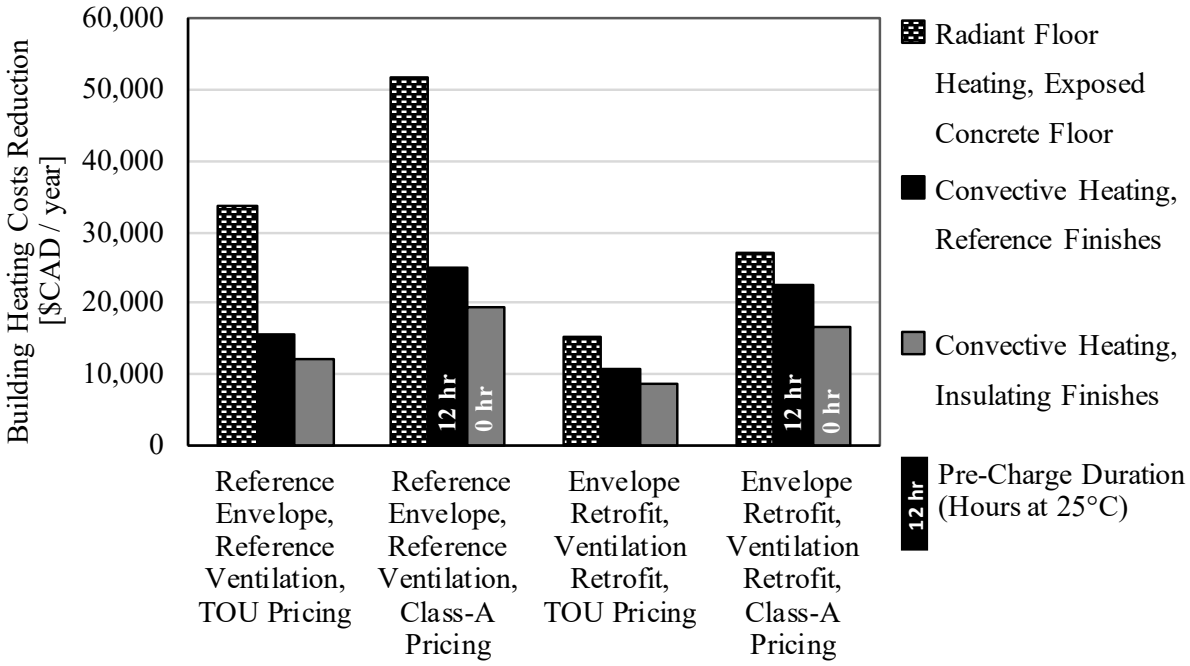

Figure 18 : The Annual Heating Cost Savings Using Load Shifting for Key Results, as Evaluated with Time-Of-Use (TOU) and Class-A Electricity Prices *

*For a 300-unit building relative to an identical model operated at 23°C, and assuming a heating system efficiency of 100%.

In Figure 18, heating cost savings for key models are shown as evaluated using both Time-Of-Use and Class-A electricity prices. The savings were calculated relative to an identical model operated at a constant setpoint temperature of 23ºC.

The greatest heating cost savings were for the models with the poorly insulated reference envelope and radiant floor heating. It was found that for models with radiant floor heating, enough thermal energy could be stored during the charging period at night that often no additional energy was required for space heating the following day. As seen in Figure 18, the benefit of this thermal storage potential was more pronounced for models with large space heating demand, such as the model with the reference envelope and the reference ventilation system. It is worth noting that the models with radiant floor also varied the thermostat setpoint within a tighter temperature band of between 22ºC and 24ºC.

As seen in Figure 18, the heating cost savings for models with convective heating systems were less than for the models with radiant floor heating systems. However, the results for convectively heated models are still important since convective heating systems are far more common in Canada. Among models with convective heating systems, it is noteworthy that the heating cost savings were not as strongly affected by building retrofits as was the case for models with radiant heating systems. Thus, for the convectively heated model with envelope and ventilation systems upgrades, the heating cost savings were very similar to the heating cost savings for convectively heated models with the reference envelope and ventilation systems. This shows that energy-efficient, convectively heated buildings might still attain significant financial savings by shifting heating demand. Further, this work showed the heating cost savings would increase substantially if residential customers were to be charged for their peak electricity demand in addition to their energy usage under the Class-A pricing scheme.

3.3 Conclusions

In this chapter, the potential benefits of shifting heating demand in existing electrically heated high-rise residential buildings in Ontario were evaluated. Shifting heating demand in electrically heated buildings facilitates the use of less expensive and less GHG-intensive electricity. An existing, 300-unit building with features typical of towers built in Ontario in the 1960s and 1970s was selected. Buildings similar to this one account for approximately 25% of housing in Toronto (Touchie 2014) and have good load shifting potential due to their compact geometry and the thermal mass of their concrete construction. The building was modeled with 16 retrofit packages to examine the importance of interior finishes, the heating system, the ventilation system, and the envelope. The models were simulated using variable suite-level temperature control to shift heating demand during both a typical year and an extremely cold night. The annual electricity cost and GHG emission savings for the model building were then evaluated using emission factors and electricity prices for Ontario.

The 16 model variants were simulated during a typical weather year to identify the building features which had the largest effect on load shifting performance, and to estimate the electricity cost and GHG emission savings currently achievable in Ontario using load shifting. It was found that the total heating demand of a model was not a good predictor of load shifting performance. Instead, load shifting performance was determined by space heating demand of the model, as only space heating demand could be shifted by varying the suite-level thermostat setpoint. Conversely, the pressurized-corridor ventilation heating demand was not affected by varying the thermostat setpoints. This meant that although retrofitting the envelope or the ventilation system had similar impacts on annual heating energy use, the impact on how much heating demand could be shifted was very different. The amount of heating demand that could be shifted was slightly increased when the pressurized-corridor ventilation system was replaced with suite-level HRVs, but was substantially reduced when the envelope was insulated and made more air-tight. The type of heating system also had a significant effect on load shifting performance during the typical year simulation. More heating demand could be shifted using radiant floors than with convective heating systems. The benefit of radiant floor heating was more pronounced for models with larger space heating demands. Of the variables considered, changes to the interior finishes were found to have the smallest effect on load shifting performance.

The annual GHG emission savings in the typical year, as evaluated with average emission factors (AEF), were between 3 Tonnes eCO_2 and 7 Tonnes eCO_2 for models with convective heating, and between 5 Tonnes eCO_2 and 20 Tonnes eCO_2 for models with radiant floor heating. Similarly, the financial savings were found to be between $8,000 and $34,000 annually using the 2018 Ontario Time-of-Use electricity prices. The GHG emission and electricity cost savings calculations were for 300-units and assumed a heating system efficiency of 100%.

The building models were also simulated during a typical Ontario peak winter electricity demand scenario. This second scenario was used to estimate the electricity cost savings that could be achieved using load shifting if residential customers in Ontario were to be charged for their contribution to peak electricity demand ($/kW) as well as their total energy usage ($/kWh). The Class-A fee structure, which is currently used for large industrial and commercial customers in Ontario, was used for the evaluation.

When charged Class-A electricity prices, greater electricity cost savings were attained for all models. The greatest electricity cost savings were attained for models with radiant floor heating and poor envelopes. For convectively heated models, the electricity cost savings were not as great as was the case for radiant floor systems, but were still significant. For convectively heated models, retrofits of the envelope or ventilation system were found to have little impact on load shifting performance during the peak winter demand event. However, the load shifting performance of convectively heated models was improved by up to 45% by optimizing interior finishes and heating the model to 25°C for 12 hours in advance of the demand peak. The building electricity cost savings were reduced between 10% and 33% compared to an identical model operated at 23ºC. For the 300-unit building models, this amounted to between $16,000 and $57,000 annually.

An important part of this study was the reference operation selected. The reference operation for this study was an identical model operated at 23ºC. The reference operation and the thermostat schedules were created based on the assumption that a model operated with a constant setpoint was comparable to the same model operated with a variable setpoint, so long as they used nearly the same amount of energy, and both were operated within the ASHRAE Standard 55 comfort boundaries.

The results indicate that several common assumptions about building operations and thermal mass are inaccurate when considering electrically heated high-rise residential buildings in Ontario. First, while it is common to reduce the setpoint at night in order to reduce energy costs, for electrically heated buildings increasing the thermostat at night could be a better way to reduce GHG emissions, reduce electricity costs, and decrease stress on the electric grid. Second, studies have indicated that, for low-energy buildings, not as much heating demand can be shifted as for less energy-efficient buildings. However, this work found that during a typical winter electricity demand peak in Ontario, the weather was cold enough that even for low-energy buildings, significant amounts of heating demand might be shifted. Third, even when considering typical heating season conditions, load shifting performance was not a function of the total annual heating demand. Rather, only the amount of space heating demand affected load shifting performance. These three insights support the importance of using realistic energy models and accurate weather data when evaluating building operation strategies.

Chapter 4
Summary of Findings and Future Work

Canadian buildings contribute significantly to GHG emissions and addressing those emissions is an important method of meeting climate action plan targets. This thesis explored two strategies for using the thermal mass of the building structures to operate buildings more sustainably. The first strategy, night ventilation, allows buildings to be cooled very efficiently. The second strategy, shifting heating demand in high-rise residential buildings with variable suite-level temperature control, enables electrically heated buildings to be heated with less expensive and less GHG-intensive electricity. While these strategies have been studied in European countries, there has been very little research on their performance in Canada.

To analyze the potential of the first strategy, a climatic analysis of Canadian cities was conducted to evaluate the feasibility of using night ventilation for cooling office buildings in summer. Since night-time temperatures are critical to the effectiveness of night ventilation, the night-time temperatures of Canadian cities were compared to the night-time temperatures of cities abroad with existing night-ventilated buildings. The results indicated that a purpose-built office building could be adequately cooled solely with night ventilation in Edmonton and Vancouver. However, night ventilation would have to be supplemented with additional cooling methods in Canadian cities with warmer night-time temperatures, such as Toronto or Montreal.

An existing high-rise residential building in Toronto was modeled with various retrofit packages in order to evaluate the potential of using variable suite-level temperature control to shift heating demand in existing buildings. The results were combined with data from the Ontario electrical grid to estimate GHG emission reductions and energy cost savings. It was found that space heating demand and the type of heating system were the most significant parameters. Given the present GHG intensity and residential price structure of electricity in Ontario, the method was found to lead to a reduction in annual heating costs of between $8,000 and $34,000 and a reduction in annual GHG emissions of between three Tonnes eCO_2 and 20 Tonnes eCO_2 for a 300-unit building. It was also found that if the electricity price structure were to be changed such that residential customers also had to pay for their peak power demand as well as paying for their energy usage, then the financial benefit of load shifting would increase.

It was found that, given optimal circumstances, both night ventilation and shifting heating demand using variable suite-level temperature control had the potential to significantly reduce GHG emissions, reduce energy costs, and reduce stress on the electrical grid. However, both strategies were significantly less effective in some of the scenarios considered. Thus, it is important to carefully consider the impact of the local climate and the building design when predicting the performance of thermal mass strategies.

The findings of this study point to several avenues that warrant further exploration. First, the climatic cooling potential (CCP) metric is limited because it does not consider the effect of night-time relative humidity. Ventilating with air near the saturation point has the potential to result in extra air-conditioning energy usage to remove unwanted moisture, and to lead to consequential moisture and moisture-induced problems. Thus, the effect of night ventilation on humidity-related areas such as indoor air quality, latent cooling loads, and building durability need to be explored.

Second, studying optimized load shifting in Ontario is potentially valuable. To create an optimized building operation schedule requires a simplified mathematical representation of a building that can be solved computationally. The results from an optimized model are a more reliable indication of the possible reduction in GHG emissions or electricity costs. Such research would therefore facilitate greater confidence in the results of this study, and might point to innovative ways of operating a building.

Finally, this research only considered one alternative electricity price structure with demand charges. However, many price structures that use demand charges are currently in use in Europe and in North America. It would be useful to examine the impact of other electricity price structures on the financial savings attained by shifting heating demand.

References

Agas G, Matsaggos T, Santamouris M, Argyriou A. 1991. On the use of the atmospheric heat sinks for heat dissipation. Energy Build. 17(4):321–329. doi:10.1016/0378-7788(91)90014-T.

Allard F, Dascalaki E, Limam K, Santamouris M. 1996. Natural Ventilation Studies within the E. C PASCOOL/JOULE II Project, International Energy Agency.

Artmann N, Jensen RL, Manz H, Heiselberg P. 2010. Experimental investigation of heat transfer during night-time ventilation. Energy Build. 42(3):366–374. doi:10.1016/j.enbuild.2009.10.003.

Artmann N, Manz H, Heiselberg P. 2007. Climatic potential for passive cooling of buildings by night-time ventilation in Europe. Appl Energy. 84(2):187–201. doi:10.1016/j.apenergy.2006.05.004.

Arundel A V., Sterling EM, Biggin JH, Sterling TD. 1986. Indirect health effects of relative humidity in indoor environments. Environ Health Perspect.

ASHRAE. 2009. Strategy 7.3 : Non-Ducted—Designed. In: In Indoor Air Quality Guide. Atlanta: American Society of Heating, Refrigerating and Air-Conditioning Engineers.

ASHRAE. 2011. 90.1 Prototype Building Models Mid-rise Apartment. https://www.energycodes.gov/901-prototype-building-models-mid-rise-apartment.

ASHRAE. 2013. ASHRAE CLIMATIC DESIGN CONDITIONS 2009/2013/2017. http://ashrae-meteo.info/.

ASHRAE. 2016. Normative Appendix G : Performance Rating Method. In: ASHRAE 90.1. Atlanta.

ASHRAE. 2017. Standard 55: Thermal Environmental Conditions For Human Occupancy. Atlanta.

Aste N, Angelotti A, Buzzetti M. 2009. The influence of the external walls thermal inertia on the energy performance of well insulated buildings. Energy Build. 41(11):1181–1187. doi:10.1016/j.enbuild.2009.06.005.

Axley JW. 2001. Application of Natural Ventilation for U. S. Commercial Buildings; Climate Suitability, Design Strategies, & Methods Modeling Studies.

Barnard N. 1996. TR4:94 - Dynamic energy storage in the building fabric.

Blondeau P, Sperandio M, Allard F. 1997. Night Ventilation for Building Cooling in Summer. Sol Energy. 61(5):327–335.

BMI. 2008. Sustainable Building Informtion Portal (German). http://www.nachhaltigesbauen.de/fileadmin/pdf/veranstaltungen/sb08/05_Energy_Optimized_Buildings.pdf.

Brager G, Borgeson S, Yoonsu L. 2007. Control strategies for mixed-mode buildings.

Braun JE. 1990. Reducing energy costs and peak electrical demand through optimal control of building thermal storage. ASHRAE Trans. 96(2):876–888.

Breesch H. 2006. Natural night ventilation in office buildings: performance evaluation based on simulation, uncertainty and sensitivity analysis.

Build Up. 2010. Natural Ventilation in Buildings - Case Studies and Design Guide. BUILD UP. [accessed 2007 Aug 20]. http://www.buildup.eu/en/node/9508.

CIBSE. 2005. Climate change and the indoor environment : impacts and adaptation. London: Chartered Institution of Building Services Engineers.

CSA. 2014. CSA-F326-M91, Residential Mechanical Ventilation Systems. Etobicoke, ON.

Döering B, Kendrick C, Lawson RM. 2013. Thermal capacity of composite floor slabs. Energy Build. 67:531–539.

Le Dréau J, Heiselberg P. 2016. Energy flexibility of residential buildings using short term heat storage in the thermal mass. Energy. 111:991–1002.

Eicker U. 2010. Cooling strategies, summer comfort and energy performance of a rehabilitated passive standard office building. Appl Energy. doi:10.1016/j.apenergy.2009.11.015.

Ellis PG, Torcellini PA. 2005. Simulating tall buildings using EnergyPlus. National Renewable Energy Lab., Golden, CO (US).

Enkvist P-A, Dinkel J, Lin C. 2010. Impact of the financial crisis on carbon economics: Version 2.1 of the global greenhouse gas abatement cost curve.

EnOB. 2011. Office buildings as investment property. https://web.archive.org/web/20111005002630/http://www.enob.info:80/en/new-buildings/project/details/office-buildings-as-investment-property/.

EnOB. 2015. Centre for Environmentally Conscious Construction. https://web.archive.org/web/20151213104633/http://www.enob.info:80/en/new-buildings/project/details/centre-for-environmentally-conscious-construction/ .

EnOB. 2016a. New Fraunhofer ISE Institute. https://web.archive.org/web/20160316030221/http://www.enob.info:80/en/new-buildings/project/details/new-fraunhofer-ise-institute/.

EnOB. 2016b. Lamparter passive office building. https://web.archive.org/web/20160315220002/http://www.enob.info/en/new-buildings/project/details/lamparter-passive-office-building/.

Environment and Climate Change Canada. 2019. Canadian Environmental Sustainability Indicators: Greenhouse gas emissions. Gatineau, Canada.

Environment Canada. 2018. Weather data by location. energyplus.net/weather-location/north_and_central_america_wmo_region_4/CAN/ON/CAN_ON_Toronto.716240_CWEC.

Eto JH. 1988. On using degree-days to account for the effects of weather on annual energy use in office buildings. Energy Build. 12(2):113–127. doi:10.1016/0378-7788(88)90073-4.

Eubanks B. 2014. Climate-Adapted Design. , May. Ashrae J.(May).

Farhat AAM, Ugursal VI. 2010. Greenhouse gas emission intensity factors for marginal electricity generation in Canada. Int J Energy Res. 34(15):1309–1327.

Foteinaki K, Li R, Heller A, Rode C. 2018. Heating system energy flexibility of low-energy residential buildings. Energy Build. 180:95–108.

Geros V, Santamouris M, Tsangrasoulis A, Guarracino G. 1999. Experimental evaluation of night ventilation phenomena. Energy Build. 29(2):141–154.

Givoni B. 1994. Passive low energy cooling of buildings. Wiley & Sons.

Hacker J, Belcher SE, YAU RMH. 2007. Climate scenarios for urban design: a case study of the London urban heat island. In: Proceedings International Conference on Climate Change (ICCC2007), Hong Kong.

Heiselberg PK. 2002. Annex 35 : HybVent - Hybrid Ventilation in New and Retrofitted Office Buildings - State of the Ar. Dept. of Building Technology and Structural Engineering, Aalborg University.

Hledik R. 2014. Rediscovering residential demand charges. Electr J. 27(7):82–96.

IESO. 2019a. Global Adjustment and Peak Demand Factor. http://www.ieso.ca/Sector-Participants/Settlements/Global-Adjustment-and-Peak-Demand-Factor.

IESO. 2019b. Top Ten Ontario Demand Peaks Archive - IESO. media/Files/IESO/settlements/Top-Ten-Ontario-Demand-Peaks-Archive.xlsx.

IESO. 2019c. Yearly HOEP OR Predispatch Report For 2018.

International Energy Agency. 1995a. Energy Conservation in Buildings and Community Systems Programme: Annex 28 - Low Energy Cooling: Review of Low Energy Technologies: Subtask 1. Ottawa.

International Energy Agency. 1995b. Annex 28 : Technical Synthesis Report. Coventry.

International Energy Agency. 1998. Annex 28 : Case Study Buildings. Dubbendorf.

Jensen SØ, Marszal-Pomianowska A, Lollini R, Pasut W, Knotzer A, Engelmann P, Stafford A, Reynders G. 2017. IEA EBC annex 67 energy flexible buildings. Energy Build. 155:25–34.

Kemp S. 2013. Ventilation and Energy Efficiency in MURBs. In: ASHRAE Ottawa Valley Chapter Meeting April.

Klein K, Herkel S, Henning H-M, Felsmann C. 2017. Load shifting using the heating and cooling system of an office building: Quantitative potential evaluation for different flexibility and storage options. Appl Energy. 203:917–937.

Kolokotroni M. 1998. Night ventilation for cooling - field tests and design tools. In: Low-Energy Cooling Technologies for Buildings. London: Professional Engineering Publishing Limited.

Krausse B, Cook M, Lomas K. 2007. Environmental performance of a naturally ventilated city centre library. Energy Build. doi:10.1016/j.enbuild.2007.02.010.

Landsman J. 2016. Performance, Prediction and Optimization of Night Ventilation across Different Climates.

Less. 2019. Offsets by the tonne.

Liu Y, Yang L, Hou L, Li S, Yang J, Wang Q. 2017. A porous building approach for modelling flow and heat transfer around and inside an isolated building on night ventilation and thermal mass. Energy. 141:1914–1927. doi:10.1016/j.energy.2017.11.137.

Ministry of Environment and Climate Change. 2016. Federal Sustainable Development Strategy. Gatineau, Canada.

NatVent. 1998. Final Monitoring Report. http://projects.bre.co.uk/natvent/reports/monitoring/final_monitor_rep.pdf.

NRCan. 2011. Energy Efficiency Trends in Canada 1990 to 2009. Ottawa.

NRCan. 2019. Energy Fact Book 2018-2019.

O'Brien W, Bourdoukan P, Delisle V, Yip S. 2015. Net ZEB design processes and tools. Model Des Optim Net-Zero Energy Build.:107–174.

O'Neill B., Shaw G, Flynn M. 1996. PROJECT PROFILE: POWERGEN HEADQUARTERS. Crowthorne.

Olesen BW. 2012. Thermo active building systems using building mass to heat and cool. Ashrae J. 54(2):44–52.

Ontario Hydro. 2018. Ontario Hydro Rates. http://www.ontario-hydro.com/current-rates.

Van Paassen AHC, Liem SH, Gröninger BP. 1998. Control of night cooling with natural ventilation.(Sensitivity Analysis of Control Strategies & Vent Openings). In: DOCUMENT-AIR INFILTRATION CENTRE AIC PROC. OSCAR FABER PLC. p. 438–447.

Pedersen TH, Hedegaard RE, Petersen S. 2017. Space heating demand response potential of retrofitted residential apartment blocks. Energy Build. 141:158–166.

Pfafferott J. 2004. Enhancing the Design and Operation of Passive Cooling Concepts. Technical University of Karlsruhe.

Pfafferott J, Herkel S, Jäschke M. 2003. Design of passive cooling by night ventilation: evaluation of a parametric model and building simulation with measurements. Energy Build. 35(11):1129–1143.

Di Placido A. 2014. A Parametric Analysis of the Thermal Performance of Concrete Floor Slabs in Cold Climates. University of Toronto.

RDH. 2013. The Importance of Slab Edge & Balcony Thermal Bridges - Report # 4: Thermal Modeling Considerations for Balconies and Various Thermal Break Strategies. Vancouver.

Ricketts L, Coughlin B, Higgins J, Finch G, Knowles W. 2017. Deep Building Enclosure Energy Retrofit Study – Final Report. Vancouver.

Ricketts L, Finch G, Bombino R. 2013. Air Leakage Control in Multi-Unit Residential Buildings. Vancouver RDH Build Eng Ltd.

Ricketts L, Straube J. 2014. Corridor pressurization system performance in multi-unit residential buildings. ASHRAE Trans. 120:J1.

Ryan NA, Johnson JX, Keoleian GA. 2016. Comparative assessment of models and methods to calculate grid electricity emissions. Environ Sci Technol. 50(17):8937–8953.

doi:10.1021/acs.est.5b05216.

De Saulles T. 2005. Thermal Mass : A concrete solution for a changing climate. Surrey.

De Saulles T. 2006. Utilization of Thermal Mass in Non-Residential Buildings. Surrey.

De Saulles T. 2012. Concrete floor solutions for passive and active cooling. Surrey.

Solgi E, Hamedani Z, Fernando R, Skates H, Orji NE. 2018. A literature review of night ventilation strategies in buildings. Energy Build. 173(June):337–352. doi:10.1016/j.enbuild.2018.05.052.

Statistics Canada. 2007. Households and the Environment: Energy Use 2007. Ottawa.

Statistics Canada. 2008. EnviroStats : Greenhouse gas emissions—a focus on Canadian households. Ottawa.

Statistics Canada. 2019. Canada at a glance : 2019. Ottawa.

TAF. 2017. A clearer view on Ontario's emissions: Practice guidelines for electricity emissions factors. Toronto.

Tassou S. 1998. Low-energy cooling technologies for buildings : challenges and opportunities for the environmental control of buildings. Professional Engineering Pub. Limited for the Institution of Mechanical Engineers.

Toftum J, Olesen BW, Kolarik J, Mattarolo L, Belkowska D. 2008. Occupant Responses and energy use in buildings with moderately drifting temperatures. American Society of Heating, Refrigerating and Air-Conditioning Engineers.

Touchie M. 2014. Improving the Energy Performance of Multi-Unit Residential Buildings Using Air-Source Heat Pumps and Enclosed Balconies. University of Toronto.

Tran T. 2013. Optimization of Natural Ventilation Design in Hot and Humid Climates Using Building Energy Simulation. University of Hawai'i.

US DOE. 2017. EnergyPlus.

US EPA. 2018. Greenhouse Gas Emissions from a Typical Passenger Vehicle.

VDI. 2015. Vdi 2078. Dusseldorf.

Voss K, Herkel S, Pfafferott J, Löhnert G, Wagner A. 2007. Energy efficient office buildings with passive cooling - Results and experiences from a research and demonstration programme. Sol Energy. 81(3):424–434. doi:10.1016/j.solener.2006.04.008.

Wagner A, Klebe M, Parker C. 2007. Monitoring results of a naturally ventilated and passively cooled office building in Frankfurt, Germany. Int J Vent. 6(1):3–20.

Walsh R, Kenny P, Brophy V. 2006. Thermal mass and sustainable building.

Warren F, Lemmen D. 2014. Canada in a Changing Climate: Sector Perspectives on Impacts and Adaptation. Ottawa.

Wilson M-A, Marchand C. 2016. Climate Change Impacts on Energy Demand Integrating Changing Temperatures into National and Regional Forecasts.

Wong S, Lévesque N, Delisle V, Gagné A, Proulx L-P. 2017. Using the thermal energy storage potential of residential homes for ToU rate savings and demand response. In: 2017 IEEE International Conference on Smart Energy Grid Engineering (SEGE). IEEE. p. 223–228.

Zimmermann M. 2003. Handbuch der passiven Kühlung. Dubbendorf: EMPA.

Appendix A : Night-Ventilated Building References

This appendix contains the references for the existing night-ventilated buildings considered in this study. These references include the weather stations used to generate the Climatic Cooling Potential (CCP) numbers. "CCP source" indicates the weather station used for temperature data, while "EPW" indicates the source of the weather file that indicated the year the data was taken from. The straight-line distance from the subject building to each weather station is also indicated. Figure A1 has the same data points as Figure 3, but the circles additionally have small grey numbers which correspond to the numbers in the "Ref" column of Table A1

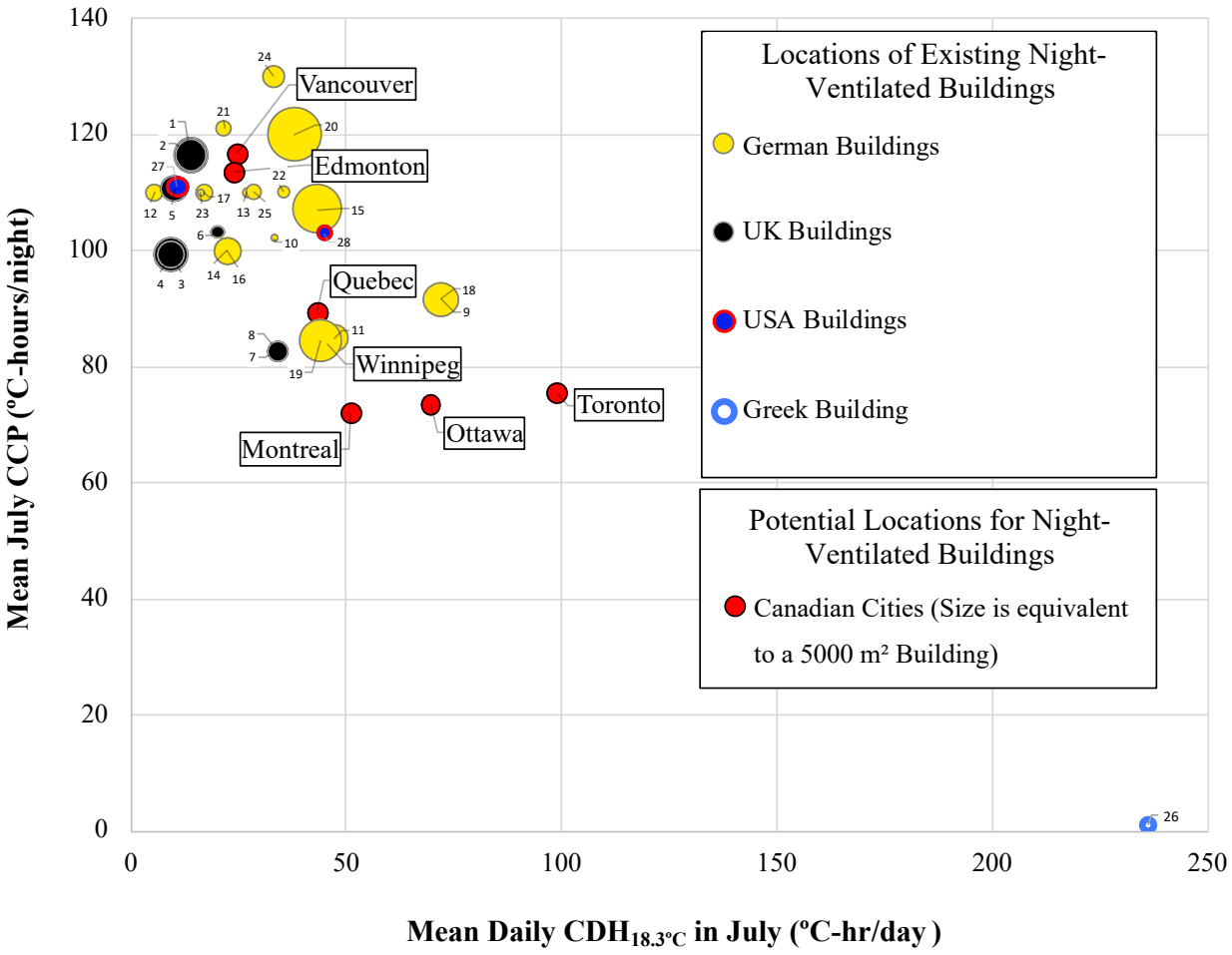

Figure A1 : References for Existing Night-Ventilated Buildings are Labelled with Small Grey Numbers

Table A1 : List of the Names, Locations, and Weather Data Sources for Existing Night-Ventilated Buildings

Ref (#)	Building Name	Source of General Building Information	Building Location	CDH Source		CCP Source		EPW Source	
				Weather Station (WMO #)	Dist. (km)	Weather Station (WMO #)	Dist. (km)	Weather Station (WMO #)	Dist. (km)
1	Toyota HQ	(De Saulles 2012)	Surrey, UK	37760	32	37760.epw	32	37760	32
2	Cannon HQ	(De Saulles 2012)	Surrey, UK	37760	32	37760.epw	32	37760	32
3	Powergen HQ	(O'Neill et al. 1996)	Coventry, UK	35440	14	35440'91	14	35340	15
4	Frederick Lancester Library	(Krausse et al. 2007)	Coventry, UK	35440	14	35440'91	14	35340	15
5	East Park Design Centre	(De Saulles 2012)	Loughborough, UK	33540	26	33540'91	26	35340	50
6	BRE building	(Kolokotroni 1998; Walsh et al. 2006)	Garston Watford, UK	36720	15	36720'97	15	37760	60
7	Bermondsey Square	(De Saulles 2012)	London, UK	37790	3	37790'97	3	37760	39
8	55 Gee Street	(De Saulles 2012)	London, UK	37790	1	37790'97	1	37760	42
9	Frauenhofer ISE	(Voss et al. 2007; BMI 2008; EnOB 2016a)	Freiburg, DE	108030	1	71900.epw	63	71900	63
10	PH office	(Eicker 2010)	Tübingen, DE	107380	21	107380.epw	21	107380	21
11	KfW Ostarkade	(Voss et al. 2007; Wagner et al. 2007; BMI 2008)	Frankfurt, DE	106370	9	106370.epw	9	106370	9
12	GIT	(Voss et al. 2007; BMI 2008)	Siegen, DE	104270	46	(Artmann et al. 2007)			
13	ZUB	(Voss et al. 2007; BMI 2008; EnOB 2015)	Kassel, DE	104380	3	(Artmann et al. 2007)			
14	Solvis	(Voss et al. 2007; BMI 2008)	Braunschweig, DE	103480	6	(Artmann et al. 2007)			
15	FH BRS	(Voss et al. 2007; BMI 2008)	St. Augustin, DE	105190	4	105130.epw	11	105130	11
16	NIZ	(Voss et al. 2007; BMI 2008)	Braunschweig, DE	103480	6	(Artmann et al. 2007)			
17	Pollmeier	(Voss et al. 2007; BMI 2008)	Creuzburg, DE	104490	39	(Artmann et al. 2007)			
18	SIC	(Voss et al. 2007; BMI 2008)	Freiburg, DE	108030	1	71900.epw	63	71900	63
19	Energieforum	(Voss et al. 2007; BMI 2008)	Berlin, DE	103840	6	103840.epw	6	103840	6
20	UBA	(Voss et al. 2007; BMI 2008)	Dessau, DE	104740	29	(Artmann et al. 2007)			
21	Ecotec	(Voss et al. 2007; BMI 2008)	Bremen, DE	102240	3	102240.epw	3	102240	3

22	Wagner	(Voss et al. 2007; BMI 2008)	Cölbe, DE	105320	31	(Artmann et al. 2007)			
23	Lamparter	(Voss et al. 2007; BMI 2008; EnOB 2016b)	Weilheim, DE	109620	10	(Artmann et al. 2007)			
24	DB Netz AG	(Voss et al. 2007; BMI 2008; EnOB 2011)	Hamm, DE	103200	45	(Artmann et al. 2007)			
25	Renson	(Breesch 2006)	Waregem, BEL	64280	18	(Artmann et al. 2007)			
26	Meletitiki	(Geros et al. 1999)	Athens Sub., GRC	167160	9	167160.epw	9	167160	9
27	La Escuelita	(Eubanks 2014; Landsman 2016)	Oakland, USA	724930	5	724930.epw	5	724930	5
28	Indio Building	(Eubanks 2014; Landsman 2016)	Sunnyvale, USA	745090	4	745090.epw	4	745090	4

Appendix B : Energy Model Inputs and Input Sources

This appendix is a detailed list of energy model inputs and their source. Data are organized according to how it would be inputted into Openstudio. Openstudio is a graphic user interface for the EnergyPlus energy modeling engine.

Table B1 : Detailed List of Energy Model Inputs and Input Sources

OpenStudio Energy Model Inputs			
Category	**Parameter**	**Model Input**	**Source, Calculation or Assumption**
General & Geometry			
	Weather File	CAN_ON_Toronto.716240_CWEC.epw CAN_ON_Toronto.716240_CWEC.ddy	
	Building Floors Modeled	1 typical floor with adiabatic B.C. (Convective) or 2 typical floors with surface matching (radiant)	
	Modeled Floor Elevation	Mid-height (85' above ground)	Drawings, Sh. 015
	Floor Area	1263 m²	EPlus Calc
	Net Total Wall Area (North/South)	718 m²	Drawings & "W/W calc"
	Net Total Wall Area (E/W)	218 m²	Drawings & "W/W calc"
	Window Area (N/S)	292 m²	
	Shading surfaces	Balconies + neighboring buildings	Drawings Sh. 008 + Google Earth measurements
Schedule Sets			
	Apt. Schedule Set	ASHRAE 90.1-2007 MidriseApartment - Apartment	Openstudio Wizard
	Corridor. Schedule Set	ASHRAE 90.1-2007 MidriseApartment - Corridor	Openstudio Wizard
	DHW Use Schedule	MNECB 1999 4.3.2.C-G	
Constructions			
	Exterior Wall - NS	Equivalent to Brick + 4" concrete block, 1.25" Insulation + gypsum board Assembly U-value 1.04 w/films	Wall section details - Sheet 018.
	Exterio Wall - EW	Equivalent to brick + 4" concrete block, 1.25" insulation + gypsum board Assembly U-value 0.925 w/films	Slab edge transmittance included into non-glazed area. Ref. RDH, 2013 "Report #4 - Thermal Modeling Considerations for Balconies and Exposed Slab Edges" U-Value w/films from eplustbl.html files.
	Exposed Concrete Floor/Ceiling	Plaster, 8" concrete, wood flooring	Drawings Sheet 018
	Interior Walls	1" plaster, 4" concrete, 1" plaster	Based on field work
	Interior Partitions	2" Sand-gypsum plaster on metal lath	Based on field work
	Window-Wall Ratio	.377 of surfaces oriented North or South	Drawings Sheet 019
	Window Type	Double-glazed, low-emissivity, aluminum thermally-broken frame U-value 2.4 , SHGC 0.4	Pg.39, Touchie, 2014 +A1:D23AHOF 2017 15.9, T4#21

Loads			
	Apartment - People	.03 ppl/m2 (Nominal)	Touchie, 2014
	Apartment - Lights	6 W/m² (Nominal)	With ASHRAE 90.1-2007 schedule., annual avg. combined consumption is 5.0W/m2 (continuos) (Touchie,2014, Pg.63). Split based on (Touchie, 2014, Appendix H)
	Apartment - Plug	4.8 W/m² (Nominal)	
	Apartment - Infiltration	0.3 ACH (Continuous)	Touchie, 2014, Appendix F
	Corridor - Lights	11 W/m² (Nominal)	2.1 times typical (Touchie, 2014, Appendix H)
	Corridor - Infiltration	0.01 ACH (Continuous)	Touchie, 2014, Appendix F
	Corridor - Ventilation	0.41 m³/s (Continuous)	Touchie, 2014, Appendix F
	Water Use	.000353 m³/s Summer, .000408 m³/s winter (Nominal)	(Touchie, 2014 Appendix H) 79 galpppd. 35-41 ppl/floor with MNECB '99 schedules.
Space Types			
	Apartment	No Ventilation. Loads, Schedules & Constructions as above.	
	Corridor	Apartment Constructions. Loads & Schedules as above.	
Thermal Zones			
	Tzones North - Equipment	Baseboard Electric &/or Constant flow hydronic, electrically heated	
	Tzones Hallway - Air Loop	Corridor MAU	
	Tzones Hallway - Thermostat	Off (T.heat=0, T.cool=50)	
	Tzones South - Equipment	Baseboard Electric &/or Constant flow hydronic, electrically heated	
HVAC Systems			
	Corridor MAU	Linked to Corridor ventilation demand	
	DHW Boiler	Autosized	
	Space Hydronic Plant		
	Service Hot Water	See DHW flowrates and schedules above	
Simulation Settings			
	Heating Sizing Factor	1.25 (ASHRAE 90.1 App.G)	Used with ASHRAE design day (ddy) data.
	Cooling Sizing Factor	1.15 (ASHRAE 90.1 App.G)	
	Timesteps per hour	6	
	Inside Convection Algorithm	TARP	
	Heat Balance Algorithm	CTF	

Appendix C : ISO 11855-2 Radiant Floor Heat Transfer Calculation

Steady-State Heat Transfer From Radiant Floor Based on ISO 1185-2:2012

Revision 2

Author: A Janusz

Objective

This objective of this calculation is to relate the supply temperature of water to a hydronic slab to the rate of steady-state heat transfer.

Assumptions

1. Constant properties of materials, through space and time

Variable Definition

$d_a := .625\ in = 0.0159\ m$ Pipe O.D.

$s_r := .001\ in = 2.54 \cdot 10^{-5}\ m$ Pipe wall thickness (.07 in)

$W := 9\ in = 0.229\ m$ Pipe spacing

$l := 400\ ft = 122\ m$ Loop length

$\lambda_b := 1.73\ \frac{watt}{m\ K}$ Concrete Conductivity (Eplus)

$\lambda_r := 0.41\ \frac{watt}{m\ K}$ PEX Conductivity (Plastic Pipe Institute TR-48/2014)

$t_{top} := 2\ in$ Toping layer thickness

$t_{below} := 8\ in$ Bottom layer thickness

$h_{top} := 5.2\ \frac{watt}{m^2\ K}$ Heat transfer coefficients, AHOF 1981,ε=0.2 because floor & ceiling mostly transmit radiation to each other.

$h_{bottom} := 2.1\ \frac{watt}{m^2\ K}$

$c_{water} := 4187\ \ (J/kg\ K)$

$pi := \pi = 3.14$

$R_{units} := \frac{1\ m^2\ K}{watt}$

$\Delta T := 8$ K, Temperature drop in Uponor video for ASHREA, 10-20degF. However, EPlus assumes total equilib, based on their modeling assumptions.

$Area_{PerTubing} := \frac{300}{400\ ft}$

$Q_{nominal} := 30$ w/m^2, nominal flowfate

$\rho_{water} := 1000\ \frac{kg}{m^3}$

$\theta_v := 29\ \Delta^\circ C$ Supply temperature

$\theta_1 := 23\ \Delta^\circ C \quad \theta_2 := \theta_1$ Room Temperature

ANALYSIS

Part A: Mass Flowrate

Here, a nominal flowrate is calculated for use in EnergyPlus and calculations below.

$$m_{dot} := \frac{1 \cdot Area_{PerTubing} \cdot Q_{nominal}}{c_{water} \cdot \Delta T} = 0.269$$ kg/s (Based on 45 W/m^2 nominal flowrate, mdot = heat load / (Water heat per flow)

$$Flow_{gpm} := \frac{m_{dot} \cdot 1\ \frac{kg}{s}}{\rho_{water}} = 4.26\ \frac{gal}{min}$$

Part B: Rate of Heat Transfer

Here, we calculte the "Virtual resistance" of a resistance network, Rt. This requires U1,U2,Rw,Rr,Rx be calculated first. Calculate the the heat transfer between imaginiary "Conductive layer" and air on the top (U1) and bottom (U2) of slab.

$$U_1 := \left(\frac{1}{\frac{1}{h_{bottom}} + \frac{t_{below}}{\lambda_b}} \right) \cdot R_{units} = 1.68 \qquad U_2 := \left(\left(\frac{1}{\frac{1}{h_{top}} + \frac{t_{top}}{\lambda_b}} \right) \right) \cdot R_{units} = 4.51$$

Rw is the film resistance, between the fluid and the pipe wall (1/h.w)

$$R_W := \left(\frac{W^{0.13}}{8 \cdot pi} \cdot \left(\frac{\left(d_a - 2 \cdot s_r \right)}{m_{dot} \cdot 1} \right)^{.87\ s^3\ kg^{-1}\ m^{-.13}\ K} \right) \cdot R_{units}^{-1} = 4.28 \cdot 10^{-5}$$

R.r is the resistance of the pipe wall.

$$R_r := \left(\frac{W \cdot \ln\left(\frac{d_a}{d_a - 2 \cdot s_r} \right)}{2 \cdot pi \cdot \lambda_r} \right) \cdot R_{units}^{-1} = 2.84 \cdot 10^{-4}$$

R.x is the resistance between the pipe wall, and the "Conductive layer"

$$R_x := \frac{\frac{W \cdot \ln\left(\frac{W}{pi \cdot d_a} \right)}{2 \cdot pi \cdot \lambda_b}}{R_{units}} = 0.032$$

Under steady-state conditions, the total resistance between the supply temp and conductive layer is:

$$R_t := \left(\frac{1}{m_{dot} \cdot c_{water} \cdot \left(1 - \exp\left(- \frac{1}{\left(R_W + R_r + R_x + \frac{1}{U_1 + U_2} \right) \cdot m_{dot} \cdot c_{water}} \right) \right)} - \frac{1}{U_1 + U_2} \right) \cdot R_{units} = 0.0328 \ \frac{m^2 \ K}{watt}$$

$$R_1 := U_1^{-1} \cdot R_{units} = 0.594 \ \frac{m^2 \ K}{watt} \qquad R_2 := U_2^{-1} \cdot R_{units} = 0.2217 \ \frac{m^2 \ K}{watt}$$

$$\theta_1 = 23 \ K \qquad \theta_2 = 23 \ K \qquad \theta_v = 29 \ K$$

$$q_1 := \left(\frac{1}{R_1 \cdot R_2 + R_1 \cdot R_t + R_2 \cdot R_t} \right) \cdot \left(R_t \cdot \left(\theta_2 - \theta_1 \right) + R_2 \cdot \left(\theta_v - \theta_1 \right) \right) = 8.4 \ \frac{watt}{m^2}$$

$$q_2 := \left(\frac{1}{R_1 \cdot R_2 + R_1 \cdot R_t + R_2 \cdot R_t} \right) \cdot \left(R_t \cdot \left(\theta_1 - \theta_2 \right) + R_1 \cdot \left(\theta_v - \theta_2 \right) \right) = 22.4966 \ \frac{watt}{m^2}$$

$$Q_{total} := q_1 + q_2 = 30.9 \ \frac{watt}{m^2}$$

$$slope := \frac{Q_{total}}{\theta_v - \theta_1} = 5.15 \ \frac{watt}{m^2 \ K}$$

Conclusion

$$slope := \frac{Q_{total}}{\theta_v - \theta_1} = 5.15 \ \frac{watt}{m^2 \ K}$$

This calculation indicates that the heat transfer to the slab is proportional to the supply temperature. IE, a 1 degree temperature differential between air temperature and water supply temperature will result in 5.15 Watts of heat gain per square meter of floor area.

Although this is only an approximation, it is consistent with the behaviour of the radiant floor model used in EnergyPlus, which makes it suitable for it's required purpose.

Appendix D : Sample Calculation for Radiant Floor Hot Water Supply Temperature

This appendix shows one example calculation of how the control parameters for the radiant floor heating were generated. This calculator provides the outdoor temperature at the maximum and minimum water supply temperature, as these are the necessary control inputs. The input variable "Floor heat output" was calculated previously according to ISO 11855-2. Other variables are from energyplus.tbl output file.

RADIANT HEATING REQUIREMENTS FOR APARTMENT ZONES - Model A-4

INPUT
OUTPUT

				Floor Area		
Height interfloor	2.67	m		total	hallway	Net
				2563	295	2268.0
Equivalent Outdoor Air						
				Floor Heat Output		
Ventilation (0, not in radiant area)	0.00	m³/s		Power=	5.15	W/m^2K
HRV eff.	0%			duty cycle	1	
Infiltration	0.30	AC/hr		Power=	**5.15**	W/m^2K
Infil. Volume	6056	m³				
TOTAL Volume	**0.50**	m³/s				
rho.air	1.3	kg/m³				
Cp.air	1000.00	J/(kg.K)				
TOTAL (Air)	**656.0**	W/K				
Equivalent Conduction						
U.window	2.402	W/m^2k	w/film			
Window area	292	m^2				
U.Wall NS	1.04	W/m^2k	w/film			
Net Area	718	m^2				
U.Wall EW	0.925	W/m^2k	w/film			
Net Area	218	m^2				
TOTAL (Conduct)	**1451**	W/K				
TOTAL (Conduction + Infiltration)	**2107**	W/K	(excluding hallway)		2267.477	
Total Heat losses per radiantly heated floor area.	**0.9**	W/m^2.K			1.0	

	Apartment Loads (Avg)		Corridor Loads (Avg)		
Avg. Lighting + Plugs	5.1	W/m^2	11	W/m^2	
Avg. People	2.7	W/m^2	0		
Avg. Solar Gain	1.06	W/m^2	0		
Indoor Temp	23	**ºC**			23
T.balancepoint	**13.52**	**ºC**			12.8

Outdoor Temp (ºC)	Supply Temp (ºC)
39	**23**
13.52	**23**
-27.69	**31**
-50.00	**31**

Appendix E : Hourly Ontario Electricity Costs, Emission Factors, Scores and Rankings

This appendix shows how the hourly GHG emissions data and electricity costs data were used to rank the hours based on their desirability for electricity use. A rank of 1 indicates that hour is the most desirable time to use electricity. These ranks were subsequently used as the basis for creating the load shifting schedules.

Table E1: Hourly Average Emission Factors, Marginal Emission Factors, Time-Of-Use Prices, and Rankings

	AEF		MEF		Time-Of-Use			
Hour	kg/kWh	Normalized	MEF: kg/kWh	Normalized	$/kWh	Normalized	Total Score:	Rank:
0	0.0377	0.74	0.0687	0.45	0.065	0.73	1.91	1
1	0.0337	0.66	0.0816	0.53	0.065	0.73	1.92	2
2	0.0325	0.64	0.1351	0.88	0.065	0.73	2.24	5
3	0.0328	0.64	0.1337	0.87	0.065	0.73	2.24	4
4	0.0344	0.67	0.1153	0.75	0.065	0.73	2.15	3
5	0.0373	0.73	0.1212	0.79	0.065	0.73	2.25	6
6	0.0411	0.80	0.1479	0.96	0.065	0.73	2.49	8
7	0.0448	0.88	0.1611	1.05	0.065	0.73	2.65	9
8	0.0479	0.94	0.1599	1.04	0.132	1.48	3.46	18
9	0.051	1.00	0.1663	1.08	0.132	1.48	3.56	19
10	0.0533	1.04	0.1921	1.25	0.132	1.48	3.77	21
11	0.055	1.08	0.2038	1.32	0.132	1.48	3.88	22
12	0.0565	1.10	0.1925	1.25	0.094	1.06	3.41	17
13	0.0571	1.12	0.1611	1.05	0.094	1.06	3.22	14
14	0.0597	1.17	0.1325	0.86	0.094	1.06	3.08	11
15	0.0614	1.20	0.136	0.88	0.094	1.06	3.14	12
16	0.0631	1.23	0.1416	0.92	0.094	1.06	3.21	13
17	0.0646	1.26	0.1506	0.98	0.094	1.06	3.30	15
18	0.0662	1.29	0.1743	1.13	0.132	1.48	3.91	23
19	0.0661	1.29	0.2073	1.35	0.132	1.48	4.12	24
20	0.0652	1.27	0.2471	1.60	0.065	0.73	3.61	20
21	0.0633	1.24	0.2112	1.37	0.065	0.73	3.34	16
22	0.057	1.11	0.1385	0.90	0.065	0.73	2.74	10
23	0.0461	0.901	0.1186	0.77	0.065	0.73	2.40	7
24	0.0377	0.737	0.0687	0.45	0.065	0.73	1.91	1

Appendix F : Methods Used to Calculate Annual Electricity Cost and Greenhouse Gas Emission Savings

This appendix provides an example of how heating costs and greenhouse gas (GHG) emissions were calculated for the annual simulations using excel.

For each building model, two simulation runs were performed in EnergyPlus. In one run, the setpoint was maintained at a constant setpoint, while for the other run the setpoint was varied to shift heating demand. Each simulation run created the raw "Heating:Electricity" output data.

Three other datasets were also required. The Average Emission Factors (AEF) and the Marginal Emission Factors (MEF) are hourly GHG data for electricity in Ontario (TAF, 2017). The Time-Of-Use (TOU) data are the hourly electricity prices for residential customers in Ontario (Ontario Hydro, 2019).

Lastly, since the simulation output is for one floor, and data are reported in Joules, conversion factors were required to make this data compatible with the units used for MEF, AEF, and TOU. These six data sets are summarized in Table F1.

Table F1 : Inputs Required for Calculating Heating Costs & Greenhouse Gas Emissions

1.	Heating Electricity EnergyPlus Data for "Model A-1" Operated at 23ºC
2.	Heating Electricity EnergyPlus Data for "Model A-1" Operated at Variable Temperature Setpoint to Shift Heating Demand
3.	Time-Of-Use Charges (TOU)
4.	Marginal Emission Factors (MEF)
5.	Average Emission Factors (AEF)
6.	Standard Unit Conversion Factors: kWh-per-Joules, Kg-per-Ton, floors-per-building

Calculating the electricity cost and GHG savings were calculated in two steps. The first step was to sum the product of each heating electricity vector with the appropriate AEF, MEF, or TOU vector and conversion factors. The total annual heating costs and GHG emissions for each model were calculated with equation [F-4] and [F-5], respectively.

$$\text{Total Heating Electricity Cost (\$)} = \frac{\text{kWh}}{Joule} \cdot \frac{\text{Floors}}{Building} \sum_{n=1}^{8760} (\text{TOU}_n \cdot \text{HE}_n) \quad \text{[F-4]}$$

Where:

TOUn = nth row of the Time-Of-Use Electricity Charge Vector ($/kWh)
HE_n = nth row of the heating electricity vector, obtained from EnergyPlus (Joules)

$$\text{Total GHG} = \frac{\text{Ton}}{kg} \cdot \frac{\text{kWh}}{Joule} \cdot \frac{\text{Floors}}{Building} \sum_{n=1}^{8760} (\text{AEF}_n \cdot \text{HE}_n) \quad \text{[F-5]}$$

Where:

Total GHG = Total annual GHG emissions due to heating electricity use (Ton)
AEF_n = nth row of the Average Emission Factor Vector (Kg / kWh)
HE_n = nth row of the heating electricity output (Joules)

In the second step, the absolute or percentage reduction in GHG emissions or heating costs were calculated using equation [F-6] or equation [F-7], respectively.

$$\text{Absolute Reduction} = \text{Total}_{\text{Load shifting}} - \text{Total}_{23°\text{C}} \quad \text{[F-6]}$$

$$\text{Percentage Reduction} = \frac{\text{Total}_{\text{Load shifting}} - \text{Total}_{23°\text{C}}}{\text{Total}_{23°\text{C}}} \quad \text{[F-7]}$$

Where:

$\text{Total}_{\text{Load shifting}}$ = Annual GHG or Heating Costs with the variable setpoint temperature

$\text{Total}_{23°\text{C}}$ = Annual GHG or Heating Costs with a constant setpoint temperature of 23ºC

Appendix G : Sample Calculations for Annual Electricity Cost and Greenhouse Gas Emission Savings

This appendix contains samples of the calculations and the data used to calculate the electricity cost and GHG emission savings.

Table G1 and Table G2 contain samples of how equations [F-4], [F-5], [F-6], and [F-7] were used. The sample calculations shown are for Model A-1. As indicated in Table 2, Model A-1 had the reference envelope, the reference ventilation system, reference finishes and electric convective heating. The model code used for “A-1” was “25-B2a”.

Table G1 : Excerpt of Spreadsheet for Calculation of Electricity Cost and Greenhouse Gas Emission Savings

	A	B	C	D	E	F	G	H	I	J	K	L	M	N	O	P	Q	R	S	T
1	Conversion Factors																			
2	Floors	20																		
3	Floor Area	1263																		
4	Kg to Tonne	0.001																		
5	kWh/Joules	2.78E-07																		
6																				
7	Inputs			Heating Energy					GHG : MEF & AEF								$: TOU			
8				Ref.		Ld Shift	Δ		Ref.		Ld Shift		Difference (Δ)				Ref.	Ld Shift	Δ	
9	Load Shift Model (Ld Shift)	Reference Model (Ref.)		(J)	(kWh/m²)	(J)	(%)		AEF (Ton CO2)	MEF (Ton CO2)	AEF (Ton CO2)	MEF (Ton CO2)	AEF (Ton CO2)	AEF (%)	MEF (%)		$	$	$	%
11	25-B2a-CO2H	25-B2a-23c		9.9E+12	108	9.9E+12	0.004%		1.4E+02	4.2E+02	1.3E+02	3.9E+02	6.8E+00	5.0%	7.0%		2.4E+05	2.3E+05	1.55E+04	6.4%
12	25-B3a-CO2H	25-B3a-23c		9.9E+12	108	9.86E+12	0.02%		1.4E+02	4.2E+02	1.3E+02	3.9E+02	7.2E+00	5.2%	7.2%		2.4E+05	2.3E+05	1.61E+04	6.7%
13	25-B4b-CO2H	25-b4b-23c		1.0E+13	111	1.00E+13	-0.3%		1.4E+02	4.2E+02	1.3E+02	4.0E+02	5.0E+00	3.6%	5.5%		2.5E+05	2.3E+05	1.22E+04	5.0%
14																				
15																				

Table G2 : Spreadsheet Formulae for Table G1

FORMULAE

Cell	Formula
D2	{=(SUM(INDIRECT("" &$B11 & "'!" & "$B$2:$B$8764")))*$B$2}
E2	=[@Column2]*B$5/($B$3*$B$2)
F2	{=SUM(INDIRECT("" &$A12 & "'!" & "B2:B8764"))*$B$2}
G2	=([@Column3]-[@Column2])/[@Column2]
I2	{=(SUM(INDIRECT(""&$B11&"'!"&"B$2:B$8761")*'AEF,MEF'!A$2:A$8761*$B$5))*$B$2*$B$4}
J2	{=(SUM(INDIRECT(""&$B11&"'!"&"B$2:B$8761")*'AEF,MEF'!B$2:B$8761*B$5))*$B$2*$B$4}
K2	{=(SUM(INDIRECT(""&$A11&"'!"&"$B$2:$B$8761")*'AEF,MEF'!$A$2:$A$8761*$B$5))*$B$2*$B$4}
L2	{=(SUM(INDIRECT(""&$A11&"'!"&"B2:B8761")*'AEF,MEF'!$B$2:$B$8761*B$5))*$B$2*$B$4}
M2	=-([@Column8]-[@Column6])
N2	=-([@Column8]-[@Column6])/[@Column6]
O2	=-(([@Column9]-[@Column62])/[@Column62])-[@Column4]
Q2	{=(SUM(INDIRECT(""&$B11&"'!"&"B$2:B$8761")*'AEF,MEF'!C$2:C$8761*B$5))*$B$2}
R2	{=(SUM(INDIRECT(""&$A11&"'!"&"$B$2:$B$8761")*'AEF,MEF'!$C$2:$C$8761*$B$5))*$B$2}
S2	=-([@Column14]-[@Column13])
T2	=-(R11-[@Column13])/[@Column13]

The formulae in Table G1 refer to three other Microsoft Excel worksheets: “25-B2-CO2H”, “25-B2-23c”, and “AEF,MEF”. Table G2 contains a sample of these worksheets. These worksheets each contain hourly data. Table G3 contains data for the 23ºC simulation, and for the simulation in which variable suite-level temperature control was used to shift heating demand. Table G4 contains the hourly price and emission intensity of electricity. Although the sample from Table G1 is a sample of the annual calculations (365 days), only the first day of the input data is included in Table G3 and Table G4.

Table G3 : First 24 Hours of Hourly Heating Electricity EnergyPlus Data for Model A-1

Constant Setpoint Run

Run ID: 25-B2a-23c

Excel Sheet ID: "25-B2a-23c"

	A	B
1	Hourly	Heating:Electricity[J]
2	2009-Jan-01 01:00:00	173814481.1
3	2009-Jan-01 02:00:00	174326824.4
4	2009-Jan-01 03:00:00	183651268.1
5	2009-Jan-01 04:00:00	190743909.5
6	2009-Jan-01 05:00:00	195214247.6
7	2009-Jan-01 06:00:00	197211965.9
8	2009-Jan-01 07:00:00	195406665.7
9	2009-Jan-01 08:00:00	194036470
10	2009-Jan-01 09:00:00	197287201.8
11	2009-Jan-01 10:00:00	196480260.2
12	2009-Jan-01 11:00:00	195445690.7
13	2009-Jan-01 12:00:00	193026081.9
14	2009-Jan-01 13:00:00	193409720
15	2009-Jan-01 14:00:00	183346286.2
16	2009-Jan-01 15:00:00	174896019.9
17	2009-Jan-01 16:00:00	170242683.3
18	2009-Jan-01 17:00:00	168118945
19	2009-Jan-01 18:00:00	168950664.6
20	2009-Jan-01 19:00:00	169631455
21	2009-Jan-01 20:00:00	172399317.1
22	2009-Jan-01 21:00:00	173029792.5
23	2009-Jan-01 22:00:00	173022109
24	2009-Jan-01 23:00:00	176568801
25	2009-Jan-02 00:00:00	180748678.6

Variable Setpoint Run

Run ID: 25-B2a-CO2H

Excel Sheet ID: 25-B2a-CO2H

	A	B
1	Hourly	Heating:Electricity[J]
2	2009-Jan-01 01:00:00	228693255
3	2009-Jan-01 02:00:00	226060670.6
4	2009-Jan-01 03:00:00	232950896.8
5	2009-Jan-01 04:00:00	237972498.2
6	2009-Jan-01 05:00:00	240549703.9
7	2009-Jan-01 06:00:00	168474666.1
8	2009-Jan-01 07:00:00	179116705.5
9	2009-Jan-01 08:00:00	179990342.1
10	2009-Jan-01 09:00:00	184716694.8
11	2009-Jan-01 10:00:00	136079170.6
12	2009-Jan-01 11:00:00	146485886.6
13	2009-Jan-01 12:00:00	146055229
14	2009-Jan-01 13:00:00	148040780.3
15	2009-Jan-01 14:00:00	193268282.7
16	2009-Jan-01 15:00:00	175772694.2
17	2009-Jan-01 16:00:00	169897254.7
18	2009-Jan-01 17:00:00	167143965.4
19	2009-Jan-01 18:00:00	114118881.2
20	2009-Jan-01 19:00:00	126010103.4
21	2009-Jan-01 20:00:00	130753574.4
22	2009-Jan-01 21:00:00	132796773.4
23	2009-Jan-01 22:00:00	240548533.8
24	2009-Jan-01 23:00:00	240747808.8
25	2009-Jan-02 00:00:00	239915790.2

Table G4 : First 24 Hours of Marginal Emission Factors, Average Emission Factors and Time-Of-Use Electricity Price Data

Excel Sheet ID: "MEF/AEF"

	A	B	C
1	AEF	MEF	$/kWh
2	**0.03370**	**0.08160**	**0.065**
3	**0.03250**	**0.13510**	**0.065**
4	**0.03280**	**0.13370**	**0.065**
5	**0.03440**	**0.11530**	**0.065**
6	**0.03730**	**0.12120**	**0.065**
7	**0.04110**	**0.14790**	**0.065**
8	**0.04480**	**0.16110**	**0.065**
9	**0.04790**	**0.15990**	**0.132**
10	**0.05100**	**0.16630**	**0.132**
11	**0.05330**	**0.19210**	**0.132**
12	**0.05500**	**0.20380**	**0.132**
13	**0.05650**	**0.19250**	**0.094**
14	**0.05710**	**0.16110**	**0.094**
15	**0.05970**	**0.13250**	**0.094**
16	**0.06140**	**0.13600**	**0.094**
17	**0.06310**	**0.14160**	**0.094**
18	**0.06460**	**0.15060**	**0.094**
19	**0.06620**	**0.17430**	**0.132**
20	**0.06610**	**0.20730**	**0.132**
21	**0.06520**	**0.24710**	**0.065**
22	**0.06330**	**0.21120**	**0.065**
23	**0.05700**	**0.13850**	**0.065**
24	**0.04610**	**0.11860**	**0.065**
25	**0.03770**	**0.06870**	**0.065**

Appendix H : Additional Simulation Results for Shifting Heating Demand During the Typical Year Scenario

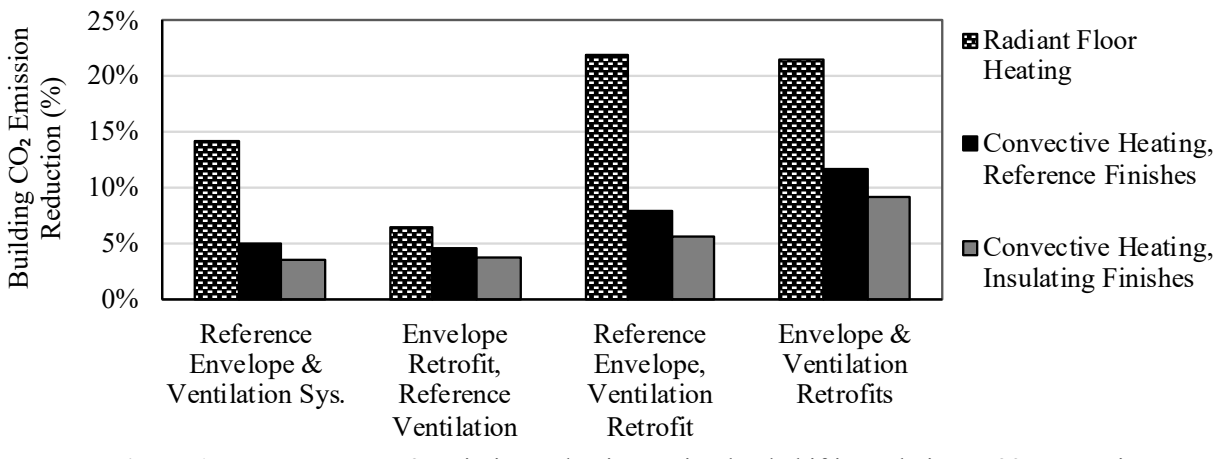

Figure H1 : Percentage Reduction in Annual Greenhouse Gas Emissions using Load Shifting and AEF for Various Retrofits*

*Using 2018 Ontario electricity data (TAF, 2017), relative to operating at 23°C

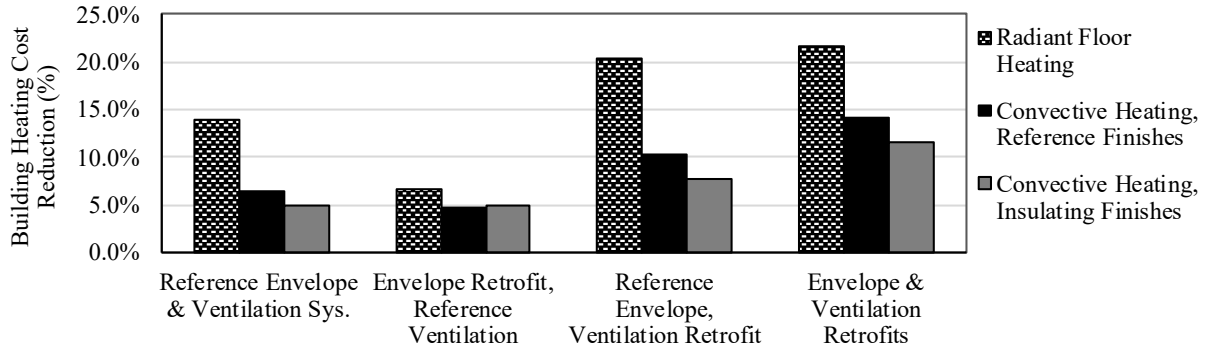

Figure H2 : Percentage Reduction in Electricity Costs Using Load Shifting and Time-of-Use Electricity Prices for Various Building Retrofits*

*Using 2018 Ontario electricity Time-of-Use prices, relative to operating at 23°C

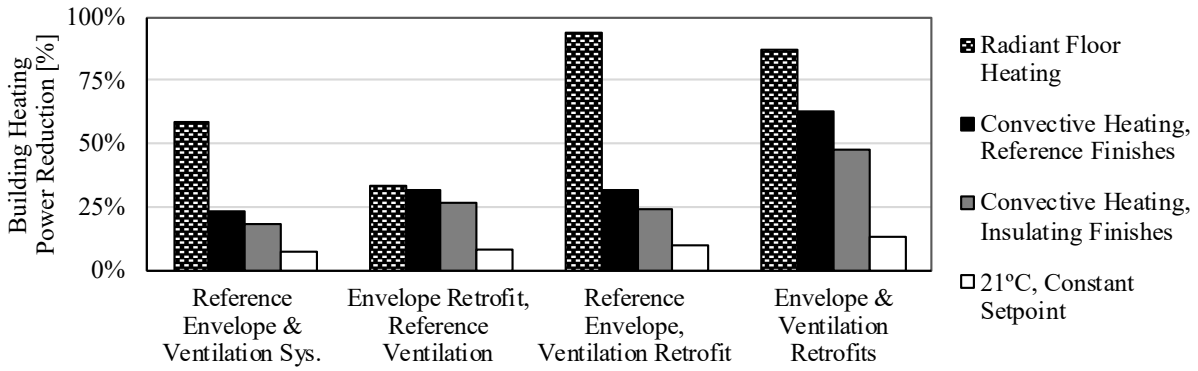

Figure H3 : Percentage Reduction in Peak Winter Electricity Demand Using Thermostat Setpoint Reduction for Various Retrofits*

* Relative to an identical building operated at 23°C, and assuming a heating system efficiency of 100%

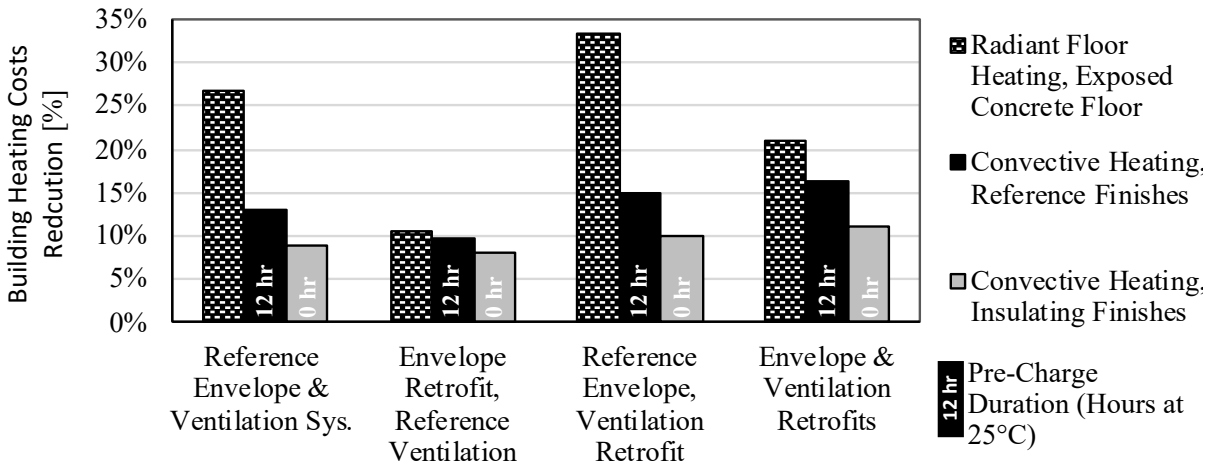

Figure H4 : Percentage Reduction in Annual Heating Costs Using Load Shifting and Class-A Electricity Prices for the Most Differentiated Combinations of Retrofits and Pre-charging Durations*

*Relative to an identical model operated at 23°C, and assuming a heating system efficiency of 100%